Supporting Information

A Simple Ternary Ion-Pair Complexation Protocol for Testing the Enantiopurity and the Absolute Configurational Analysis of Acids and Ester Derivatives

Neeru Arya, Sandeep Kumar Mishra and N Suryaprakash*

NMR Research Centre and Solid State and Structural Chemistry Unit, Indian Institute of Science, Bangalore 560012, India.

E-mail: nsp@iisc.ac.in; suryaprakash1703@gmail.com ; Fax: +91 8023601550; Tel: +91 8023607344; +91 80 22933300; +919845124802 (Cell)

Table of Contents

Fig. S12: 400 MHz ^{1}H-NMR spectrum of (*S*)-BINAM, (*S*)-(+)-2-hydroxy-3-methylbutyric acid and TFMS in $CDCl_3$

Fig. S13: 400 MHz ^{1}H-NMR spectrum of (*R*)-BINAM, (*S*)-(+)-α-hydroxy-1,3-dioxo-2-isoisoindolinebutyric acid and TFMS in $CDCl_3$

Fig. S14: 400 MHz ^{1}H-NMR spectrum of (*S*)-BINAM, (*S*)-(+)-α-hydroxy-1,3-dioxo-2-isoisoindolinebutyric acid and TFMS in $CDCl_3$

Fig. S15: 400 MHz ^{1}H-NMR spectrum of (*R*)-BINAM, (*S*)-(-)-3-hydroxy-3,3-dimethylbutanoic acid and TFMS in $CDCl_3$

Fig. S16: 400 MHz ^{1}H-NMR spectrum of (*S*)-BINAM, (*S*)-(-)-3-hydroxy-3,3-dimethylbutanoic acid and TFMS in $CDCl_3$

Fig. S17: 400 MHz ^{1}H-NMR spectrum of (*R*)-BINAM, (*L*)-(-)-3-phenyllactic acid and TFMS in $CDCl_3$

Fig. S18: 400 MHz ^{1}H-NMR spectrum of (*S*)-BINAM, (*L*)-(-)-3-phenyllactic acid and TFMS in $CDCl_3$

Fig. S19: 400 MHz ^{1}H-NMR spectrum of (*R*)-BINAM, (*S*)-(+)-α-methoxyphenylacetic acid and TFMS in $CDCl_3$

Fig. S20: 400 MHz ^{1}H-NMR spectrum of (*S*)-BINAM, (*S*)-(+)-α-methoxyphenylacetic acid and TFMS in $CDCl_3$

Fig. S21: 400 MHz ^{1}H-NMR spectrum of (*R*)-BINAM, (*R*)-(-)-α-methoxyphenylacetic acid and TFMS in $CDCl_3$

Fig. S22: 400 MHz ^{1}H-NMR spectrum of (*S*)-BINAM, (*R*)-(-)-α-methoxyphenylacetic acid and TFMS in $CDCl_3$

Fig. S23: 400 MHz ^{1}H-NMR spectrum of (*R*)-BINAM, Methyl (2*S*,3*R*) -(-)-2,3-dihydroxy-3-phenylpropionate and TFMS in $CDCl_3$

Fig. S24: 400 MHz ^{1}H-NMR spectrum of (*S*)-BINAM, Methyl (2*S*,3*R*) -(-)-2,3-dihydroxy-3-phenylpropionate and TFMS in $CDCl_3$

Fig. S25: 400 MHz ^{1}H-NMR spectrum of (*R*)-BINAM, Methyl (2*R*,3*S*) -(+)-2,3-dihydroxy-3-phenylpropionate and TFMS in $CDCl_3$

Fig. S26: 400 MHz ^{1}H-NMR spectrum of (*S*)-BINAM, Methyl (2*R*,3*S*) -(+)-2,3-dihydroxy-3-phenylpropionate and TFMS in $CDCl_3$

Fig. S27: 400 MHz ^{1}H-NMR spectrum of (*R*)-BINAM, (*R*)-pyrrolidine-2-carboxylic acid methyl ester and TFMS in $CDCl_3$

Fig. S28: 400 MHz ^{1}H-NMR spectrum of (*S*)-BINAM, (*R*)-pyrrolidine-2-carboxylic acid methyl ester and TFMS in $CDCl_3$

Fig. S29: 400 MHz ^{1}H-NMR spectrum of (*R*)-BINAM, Benzyl (*R*)-(-)-mandelate and TFMS in $CDCl_3$

Coordinates for (*S*)-BINAM/ (*S*)-Mandelic acid/ TFMS complex (Gaussian 09)

Reference

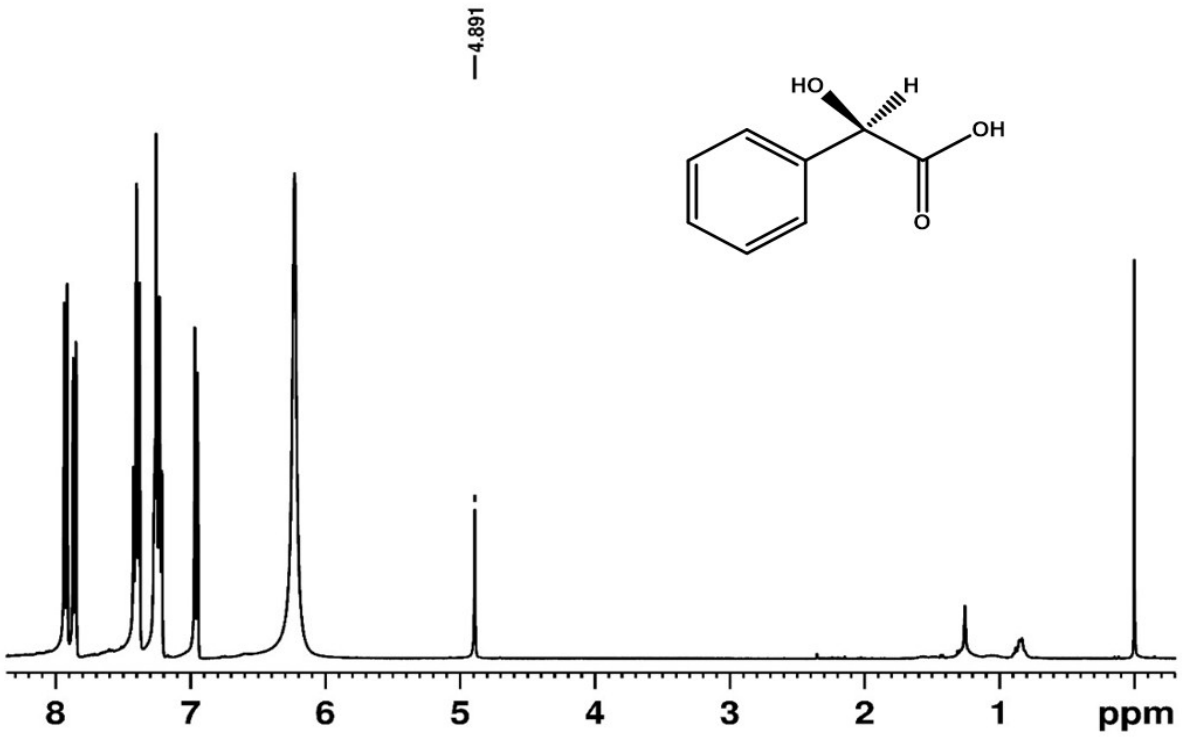

Fig.S1: 400 MHz ^{1}H-NMR spectrum of (*R*)-BINAM, (*R*)-Mandelic acid and TFMS in $CDCl_3$.

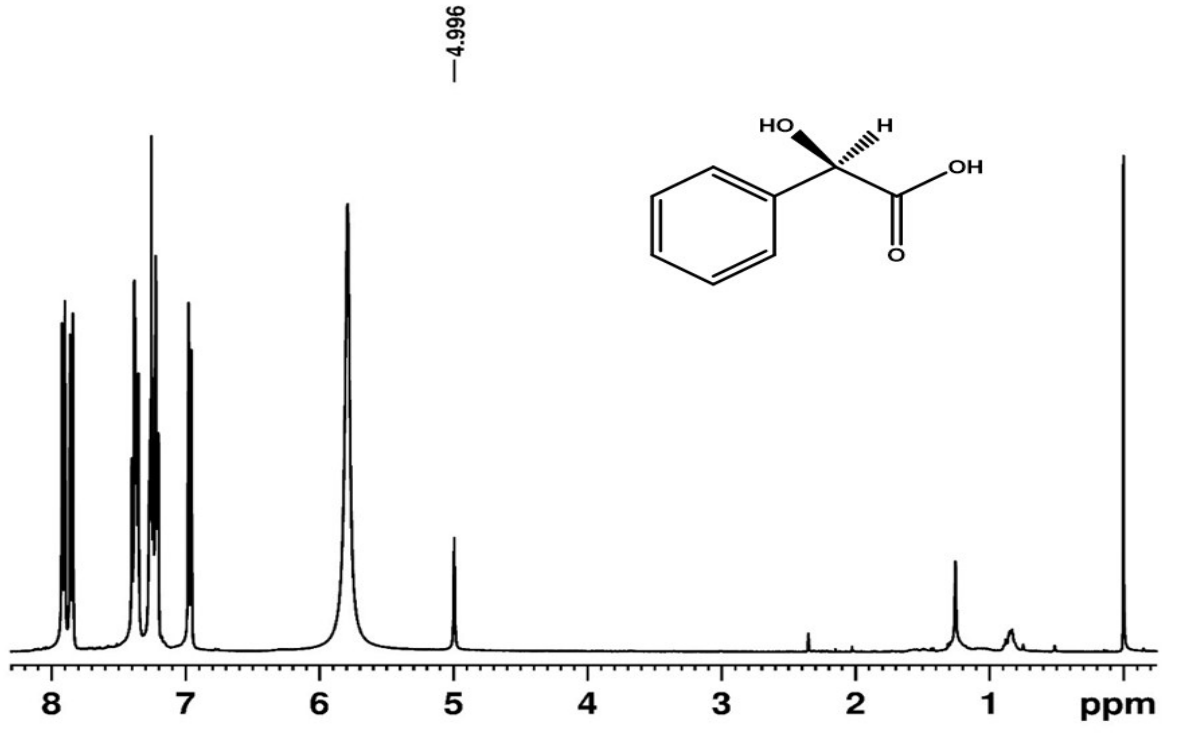

Fig.S2: 400 MHz ^{1}H-NMR spectrum of (*S*)-BINAM, (*R*)-Mandelic acid and TFMS in $CDCl_3$.

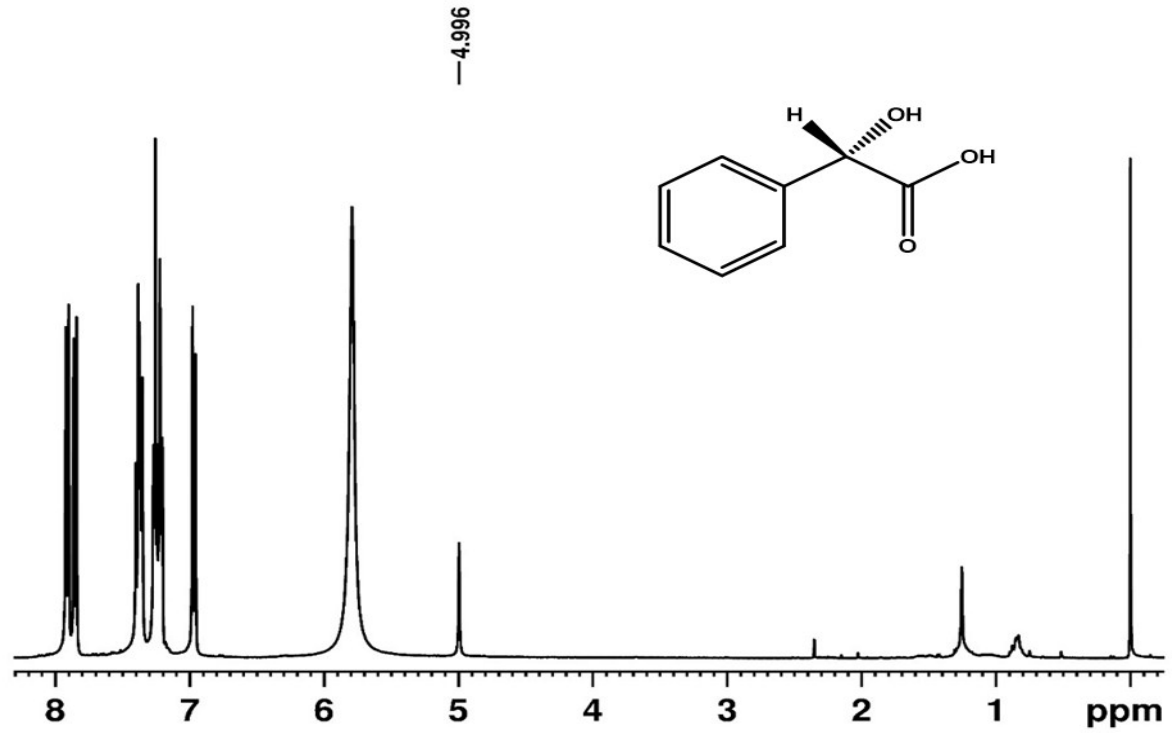

Fig. S3: 400 MHz ^{1}H-NMR spectrum of (*R*)-BINAM, (*S*)-Mandelic acid and TFMS in $CDCl_3$.

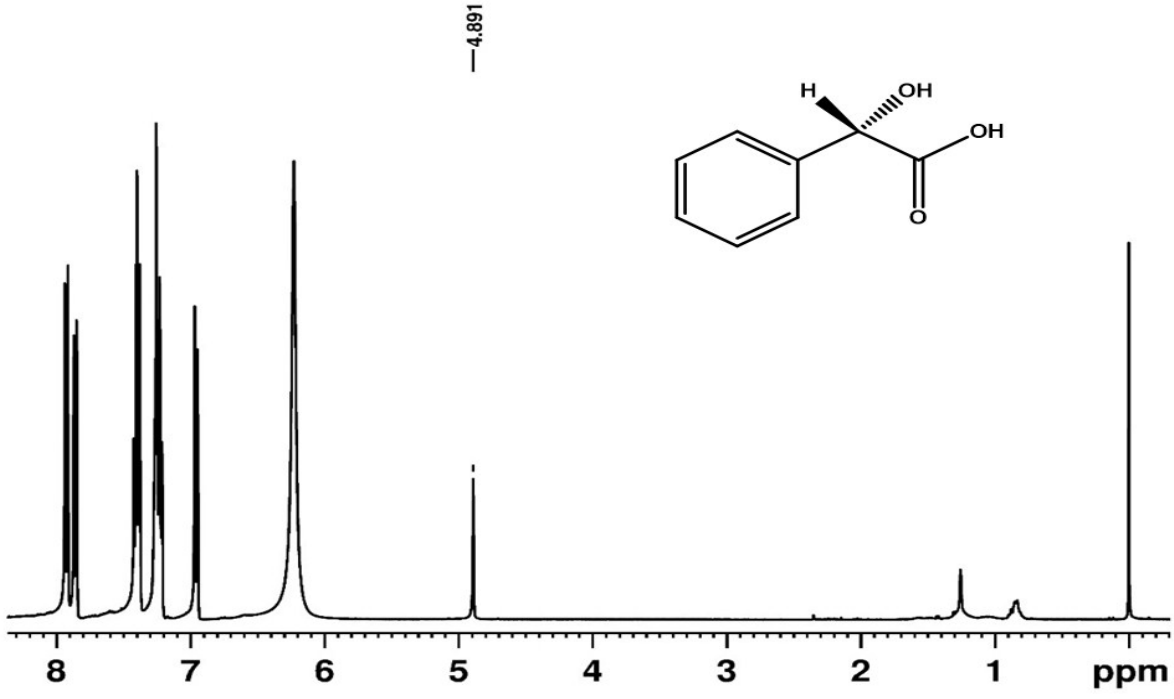

Fig. S4: 400 MHz ^{1}H-NMR spectrum of (*S*)-BINAM, (*S*)-Mandelic acid and TFMS in $CDCl_3$.

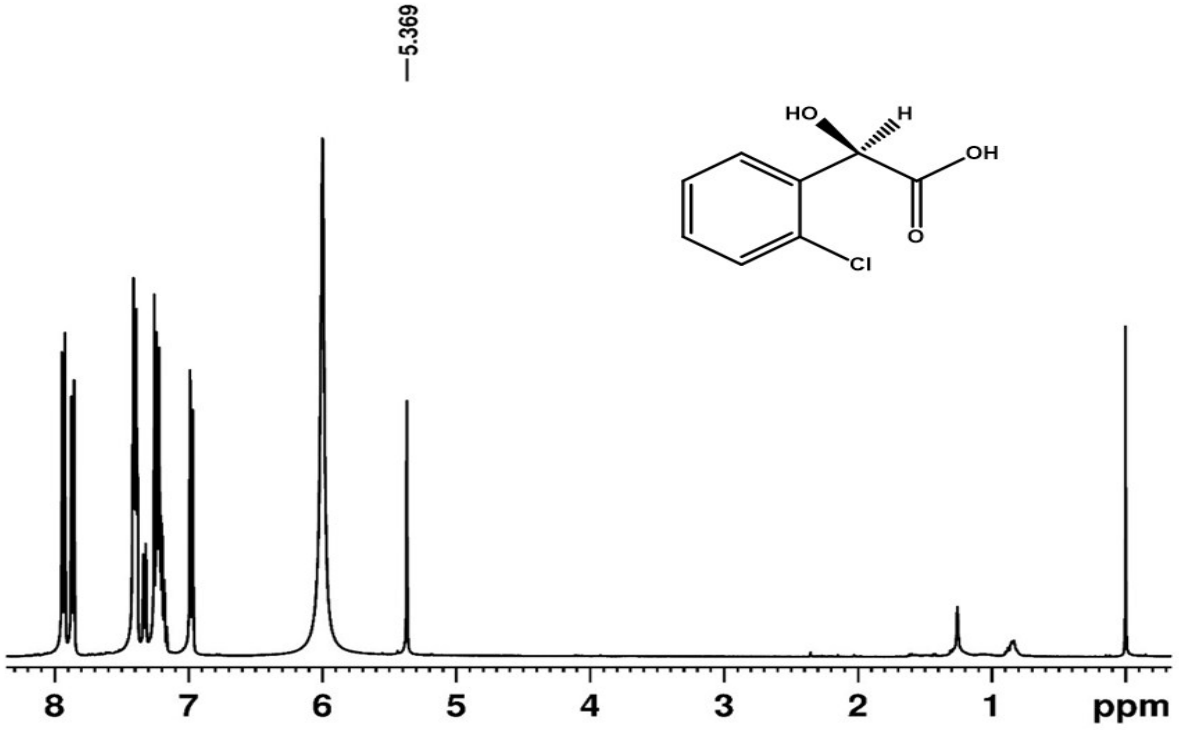

Fig. S5: 400 MHz ^{1}H-NMR spectrum of (*R*)-BINAM, (*R*)-(-)-2-chloromandelic acid and TFMS in $CDCl_3$.

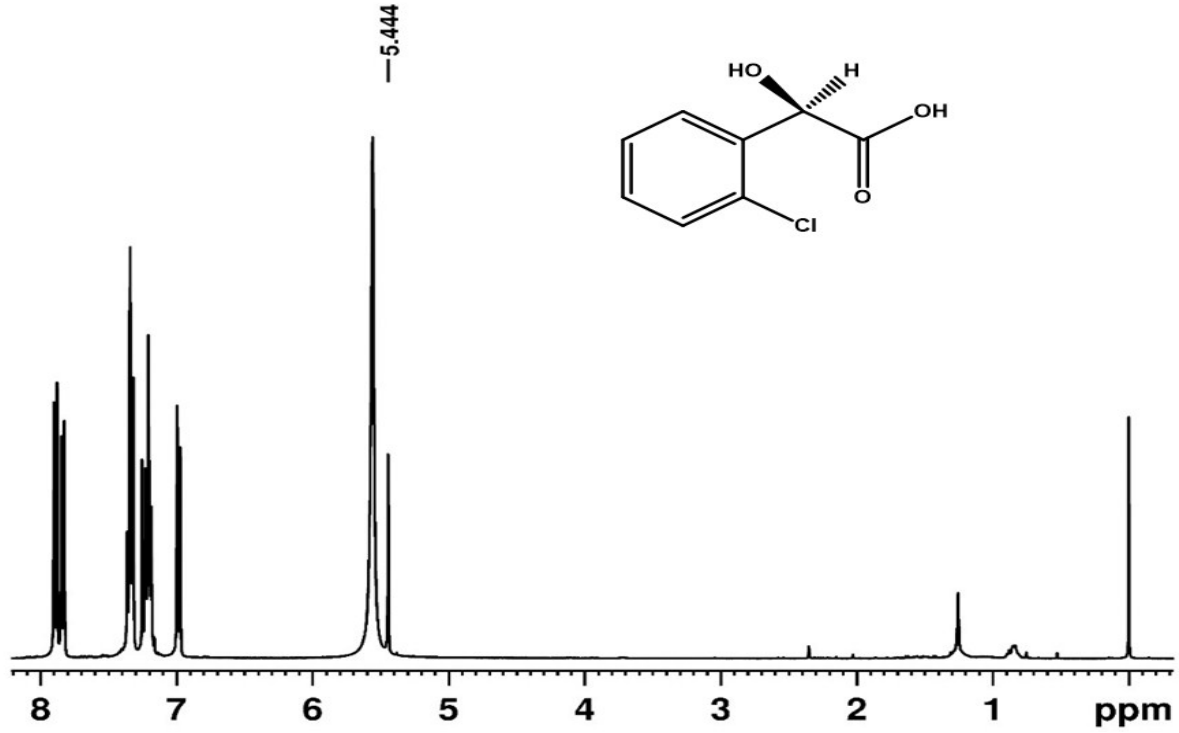

Fig. S6: 400 MHz ^{1}H-NMR spectrum of (*S*)-BINAM, (*R*)-(-)-2-chloromandelic acid and TFMS in $CDCl_3$.

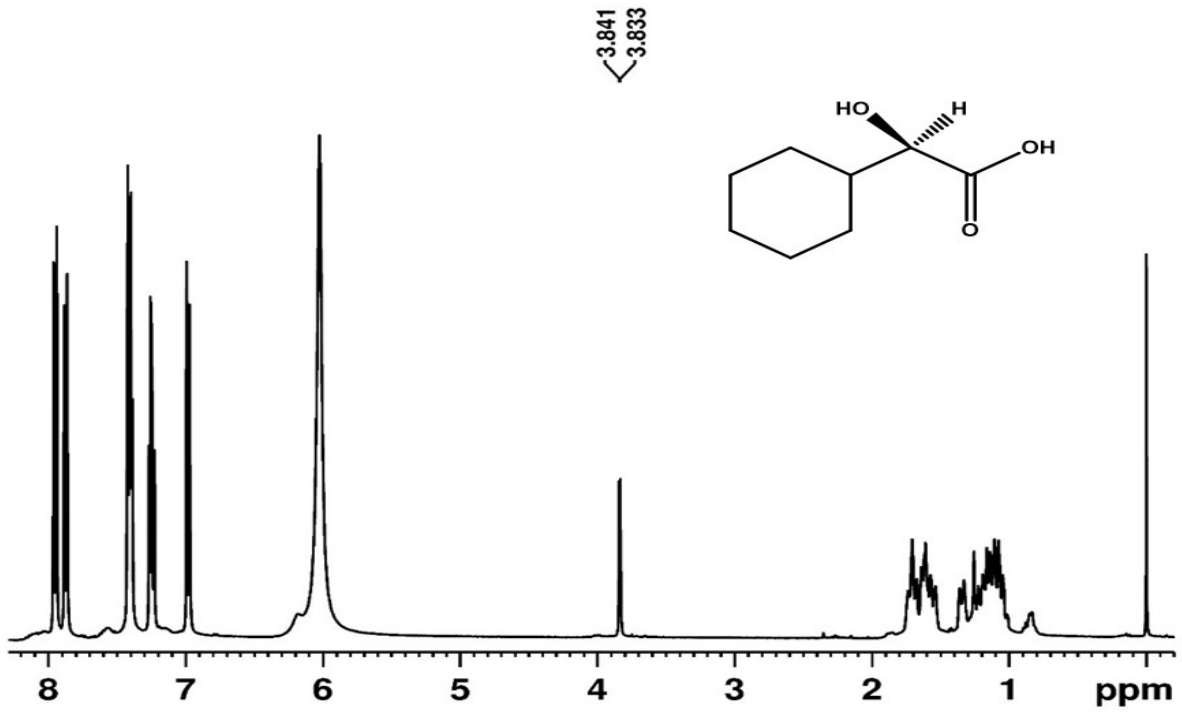

Fig. S7: 400 MHz ^{1}H-NMR spectrum of (*R*)-BINAM, (*R*)- (-) hexahydroxymandelic acid and TFMS in $CDCl_3$.

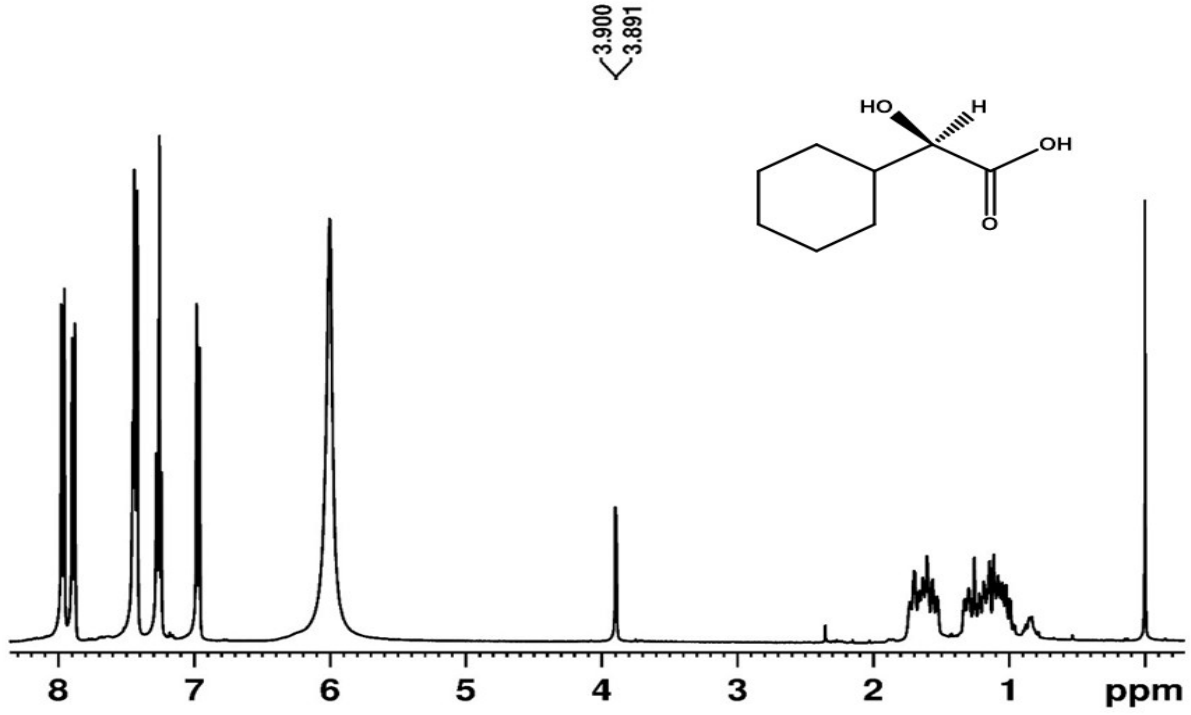

Fig. S8: 400 MHz ^{1}H-NMR spectrum of (*S*)-BINAM, (*R*)- (-)-hexahydrxyomandelic acid and TFMS in $CDCl_3$.

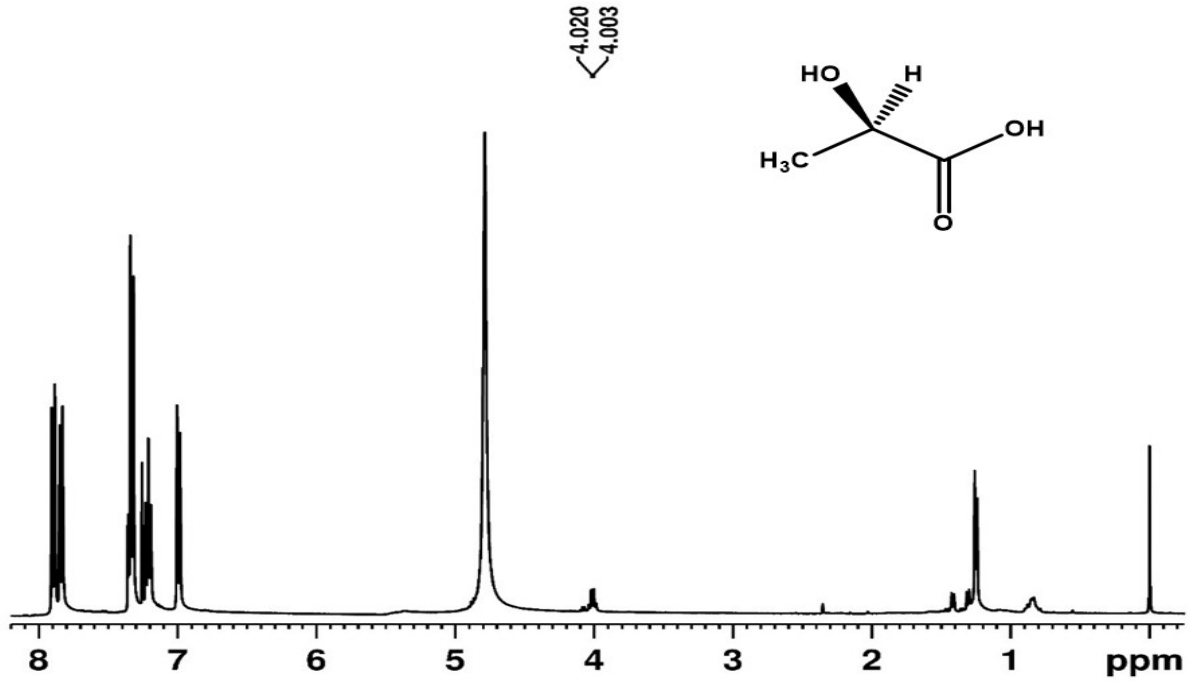

Fig. S9: 400 MHz ^{1}H-NMR spectrum of (*R*)-BINAM, (*L*)-(+)-lactic acid and TFMS in $CDCl_3$.

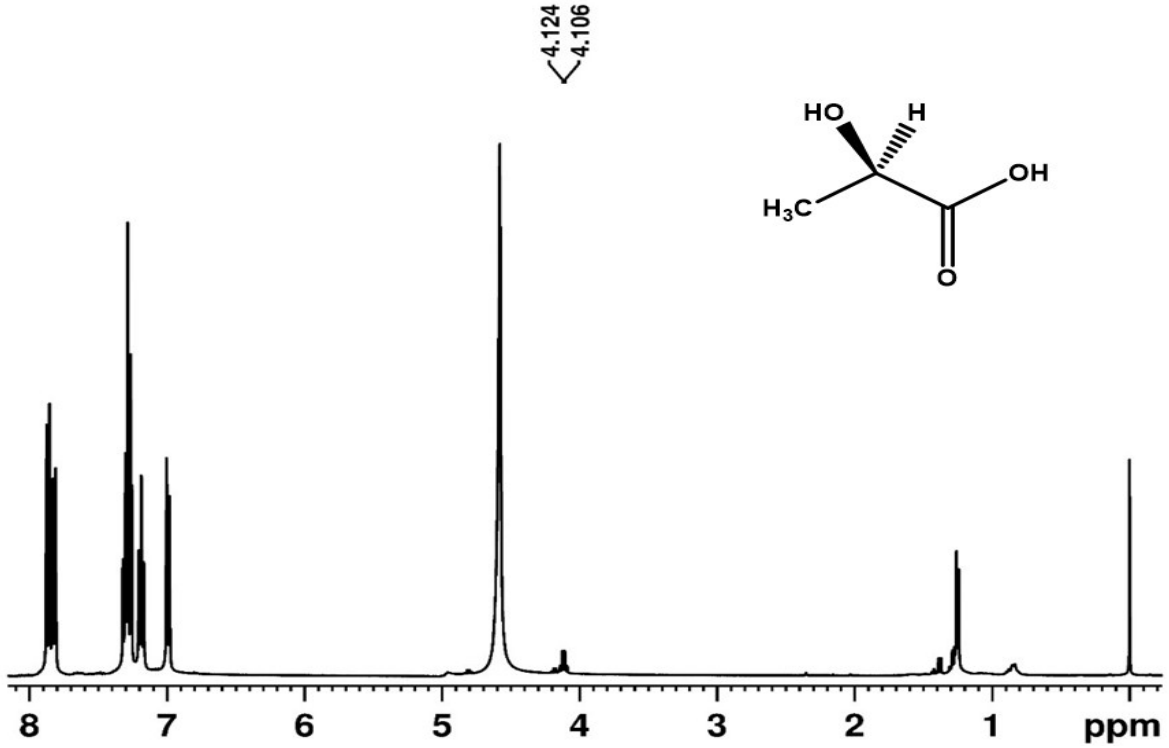

Fig. S10: 400 MHz ^{1}H-NMR spectrum of (*S*)-BINAM, (*L*)-(+)-lactic acid and TFMS in $CDCl_3$

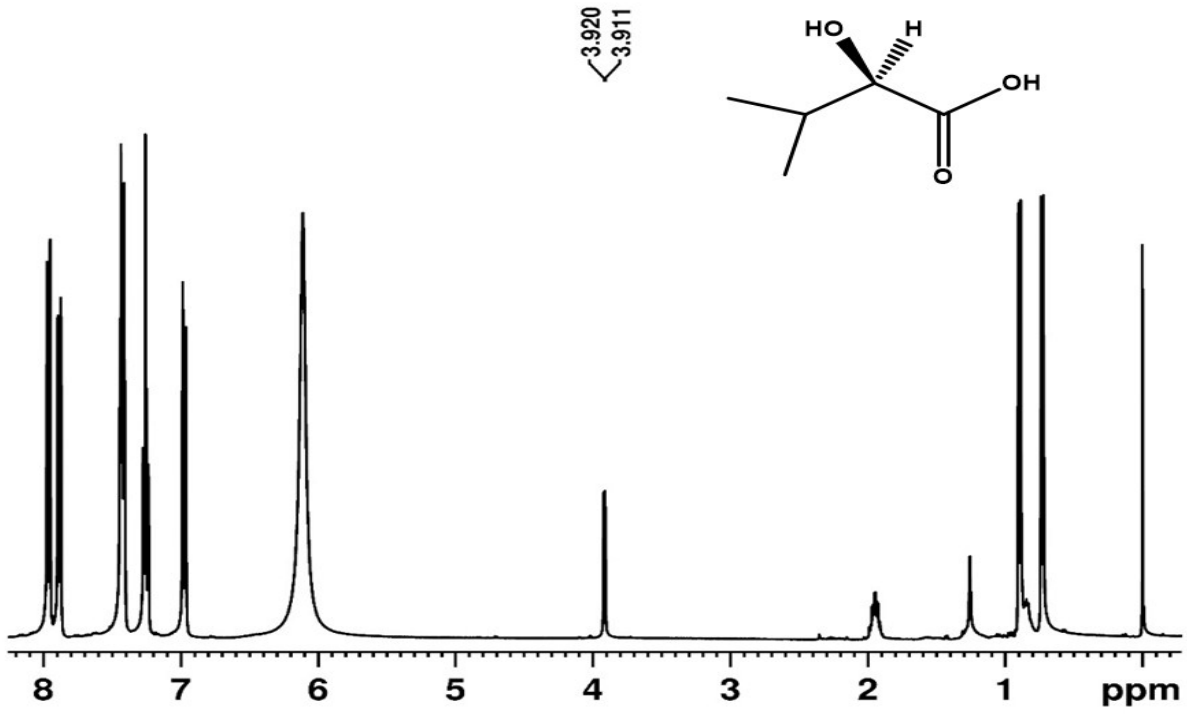

Fig. S11: 400 MHz ^{1}H-NMR spectrum of (*R*)-BINAM, (*S*)-(+)-2-hydroxy-3-methylbutyric acid and TFMS in $CDCl_3$

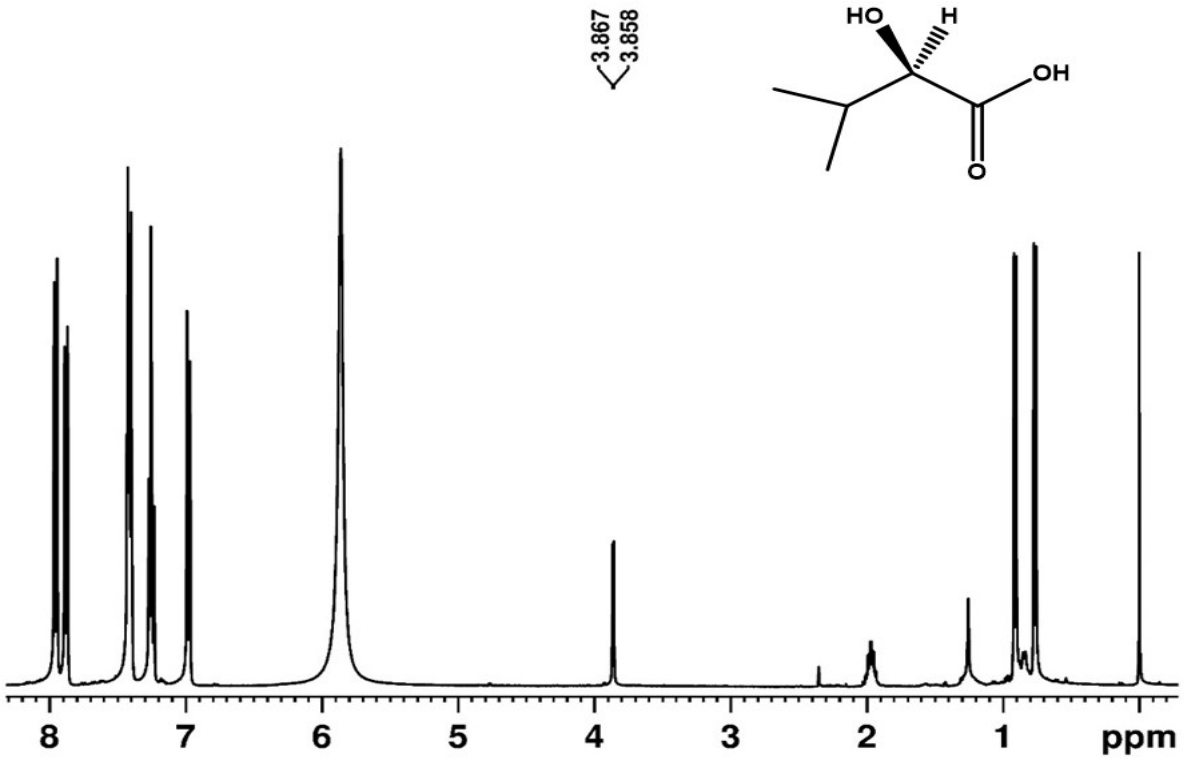

Fig. S12: 400 MHz ^{1}H-NMR spectrum of (*S*)-BINAM, (*S*)-(+)-2-hydroxy-3-methylbutyric acid and TFMS in $CDCl_3$

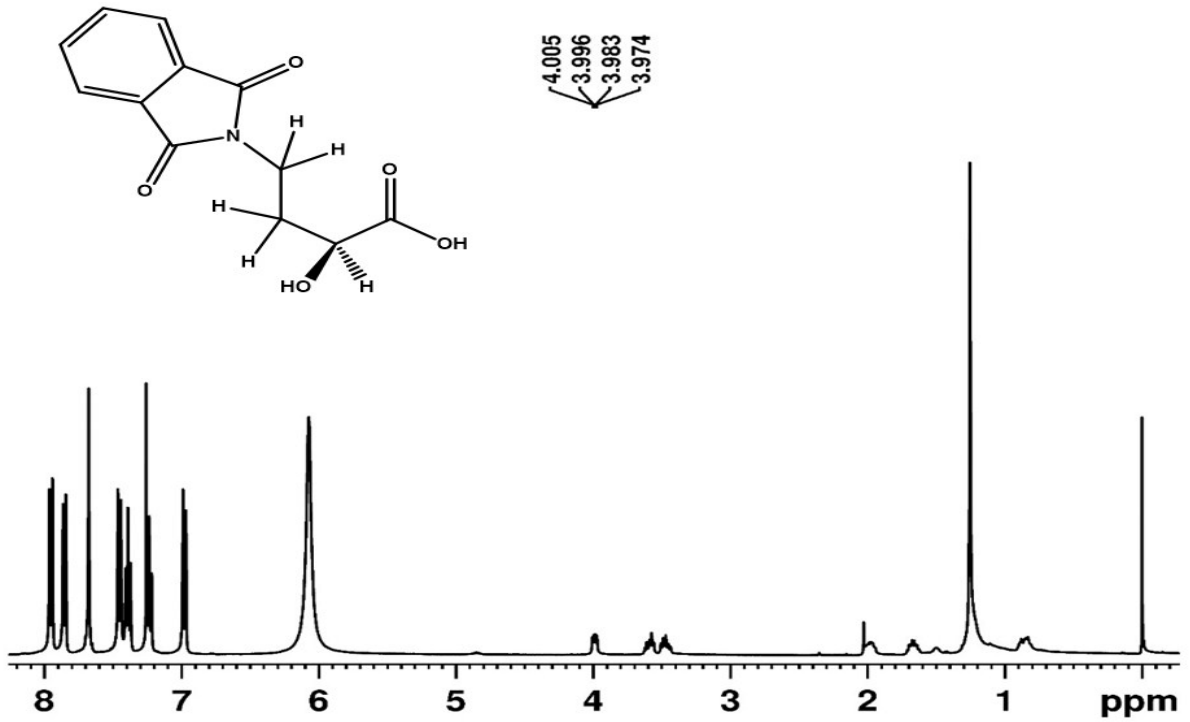

Fig. S13: 400 MHz ^{1}H-NMR spectrum of (*R*)-BINAM, (*S*)-(+)-α-hydroxy-1,3-dioxo-2-isoisoindolinebutyric acid and TFMS in $CDCl_3$

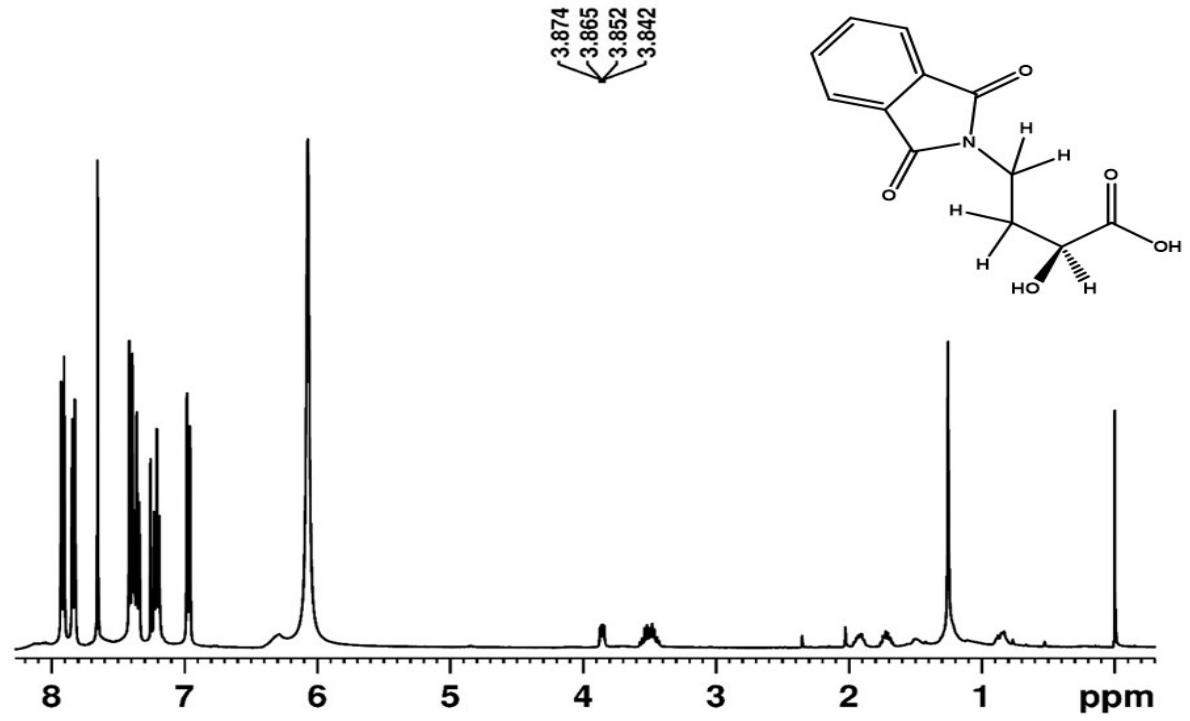

Fig. S14: 400 MHz ^{1}H-NMR spectrum of (*S*)-BINAM, (*S*)-(+)-α-hydroxy-1,3-dioxo-2-isoisoindolinebutyric acid and TFMS in $CDCl_3$

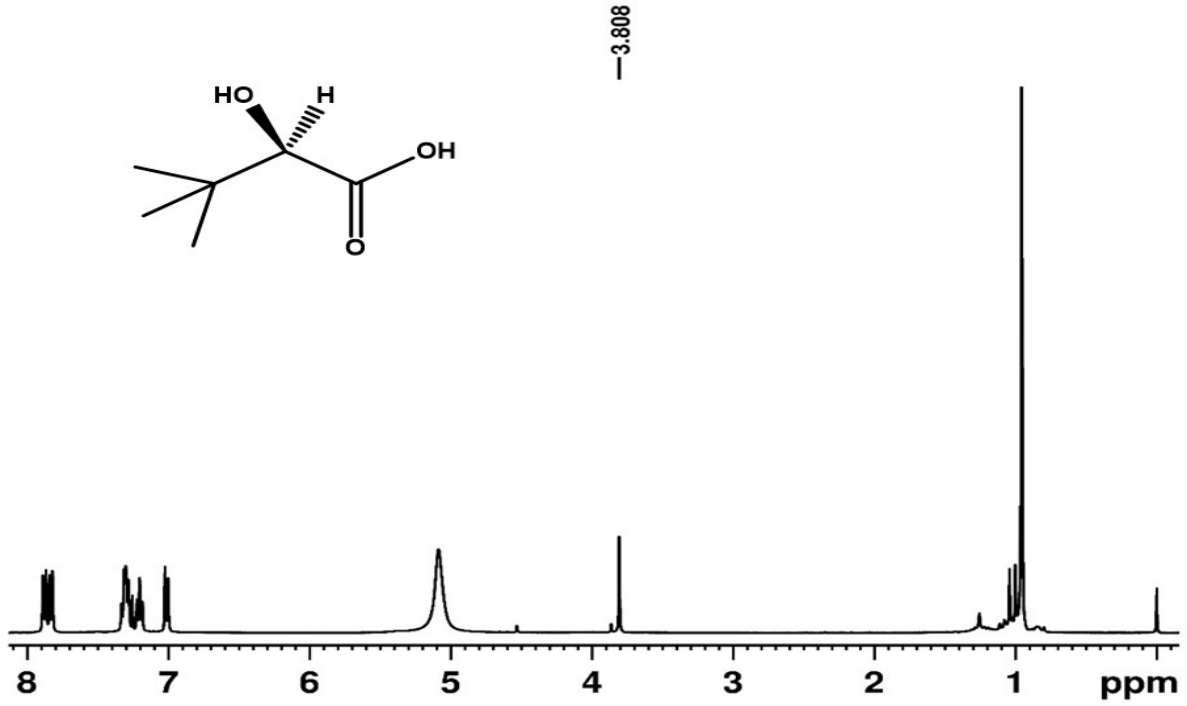

Fig. S15: 400 MHz ^{1}H-NMR spectrum of (*R*)-BINAM, (*S*)-(-)-3-hydroxy-3,3 dimethylbutanoic acid and TFMS in $CDCl_3$

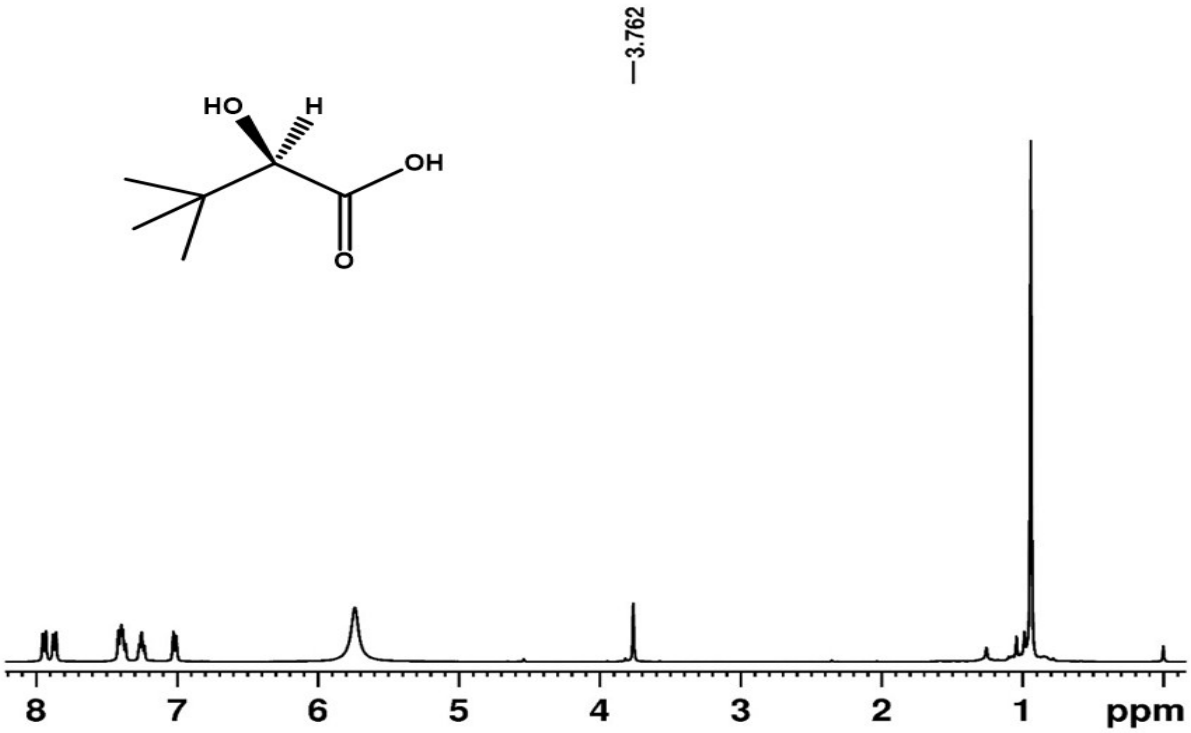

Fig. S16: 400 MHz ^{1}H-NMR spectrum of (*S*)-BINAM, (*S*)-(-)-3-hydroxy-3,3 dimethylbutanoic acid and TFMS in $CDCl_3$

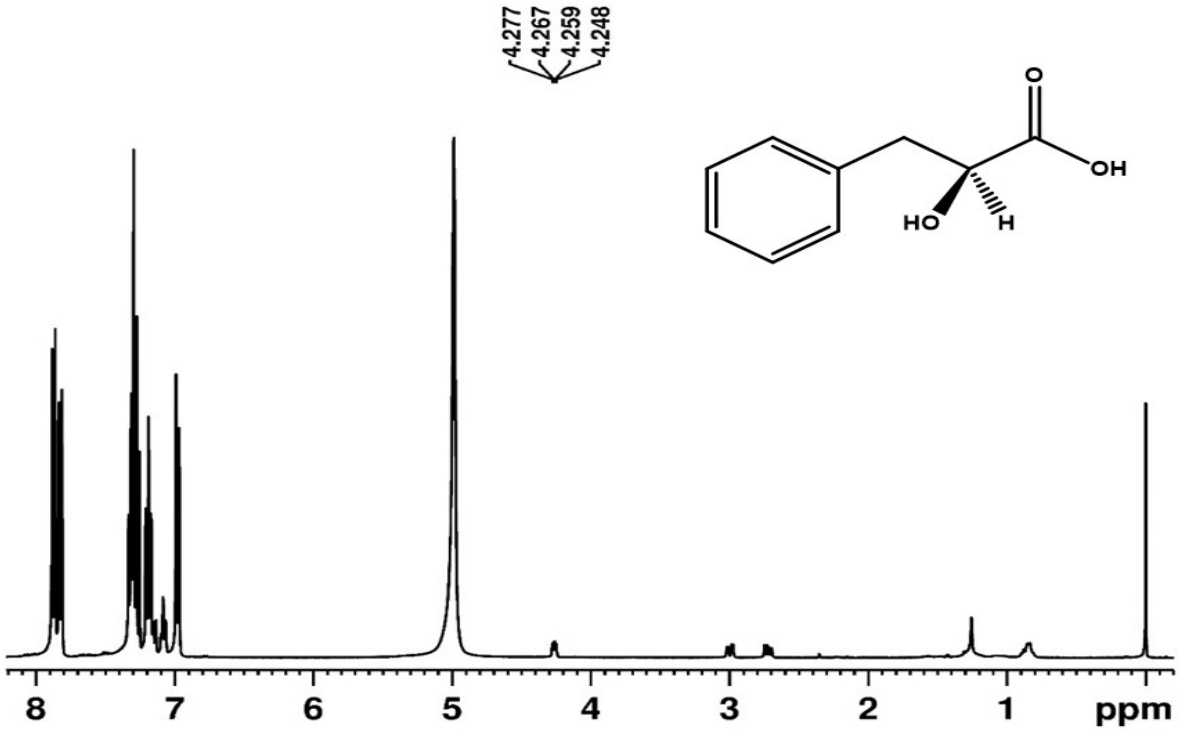

Fig. S17: 400 MHz ^{1}H-NMR spectrum of (*R*)-BINAM, (*L*)-(-)-3-phenyllactic acid and TFMS in $CDCl_3$

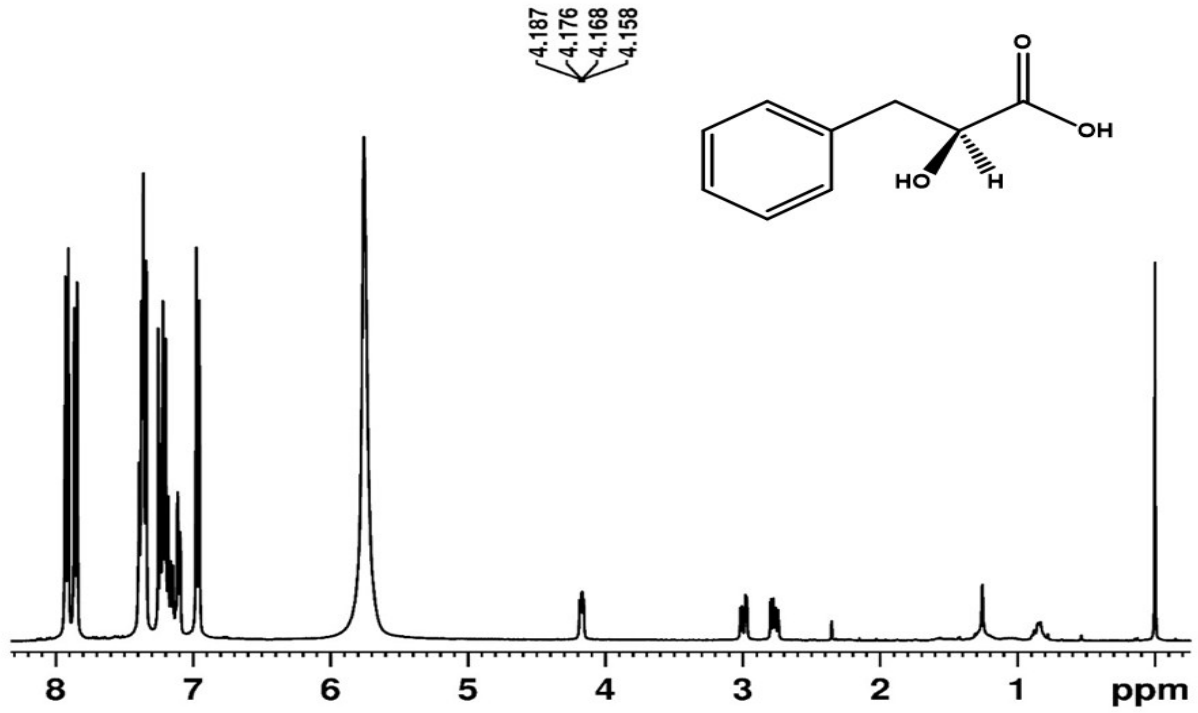

Fig. S18: 400 MHz ^{1}H-NMR spectrum of (*S*)-BINAM, (*L*)-(-)-3-phenyllactic acid and TFMS in $CDCl_3$

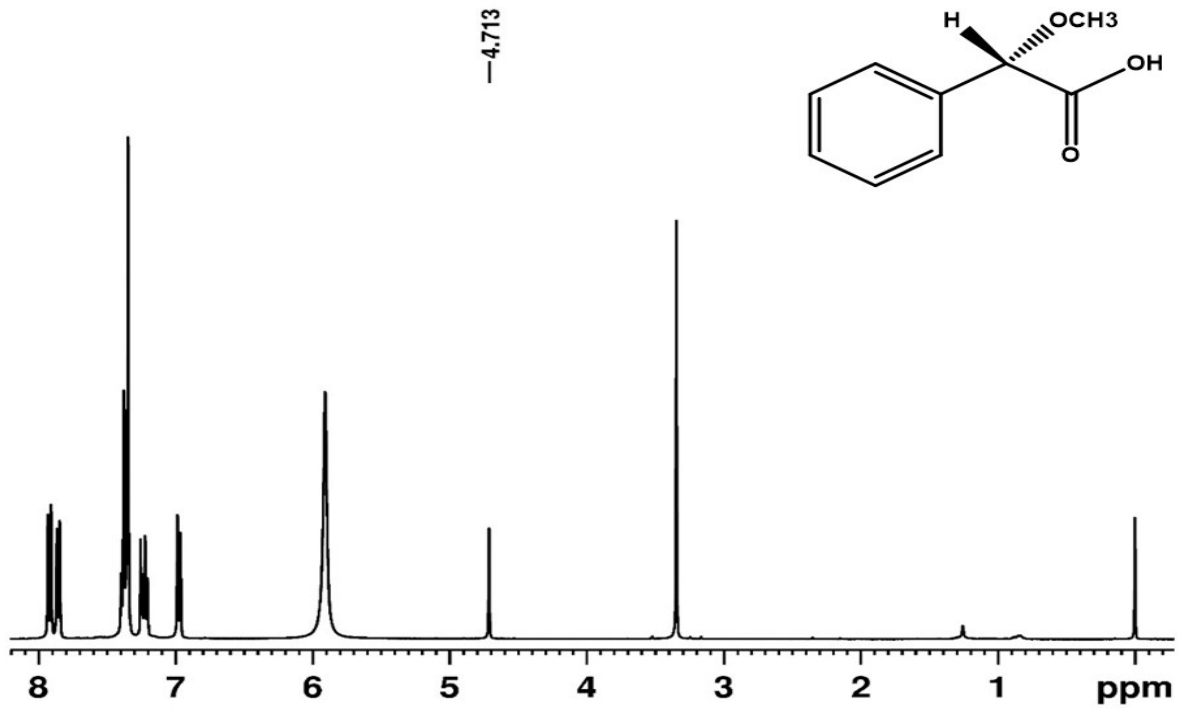

Fig. S19: 400 MHz ^{1}H-NMR spectrum of (*R*)-BINAM, (*S*)-(+)-α-methoxyphenylacetic acid and TFMS in $CDCl_3$

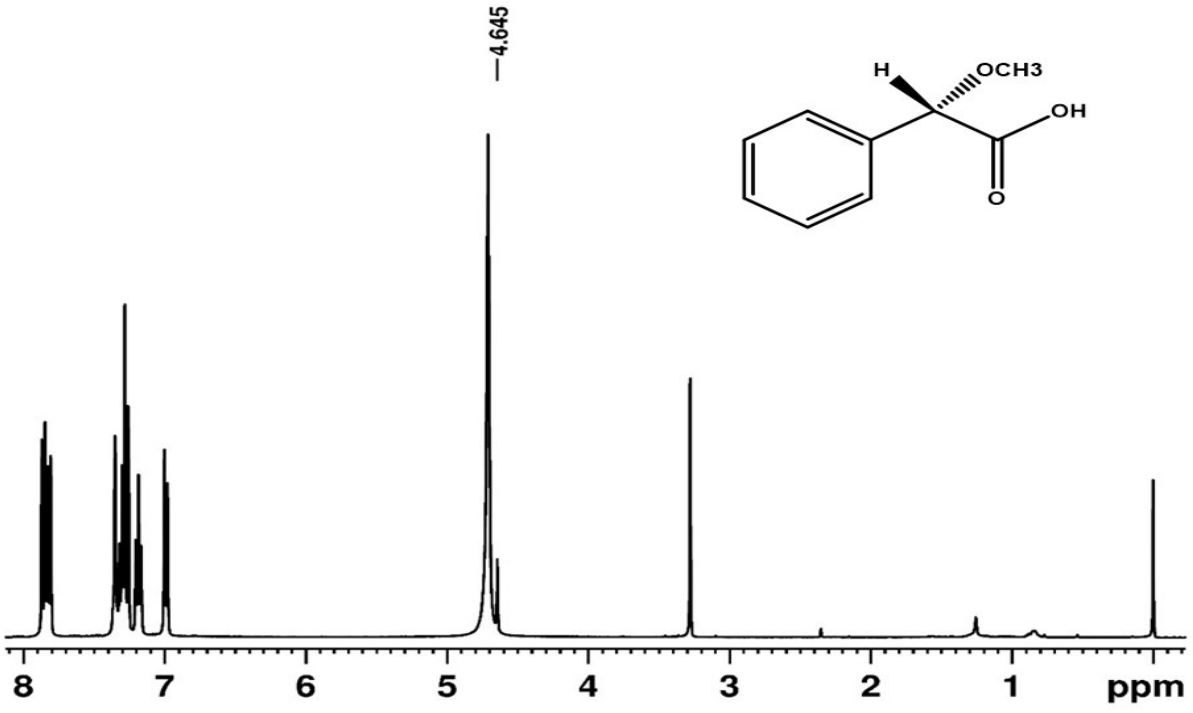

Fig. S20: 400 MHz ^{1}H-NMR spectrum of (*S*)-BINAM, (*S*)-(+)-α-methoxyphenylacetic acid and TFMS in $CDCl_3$

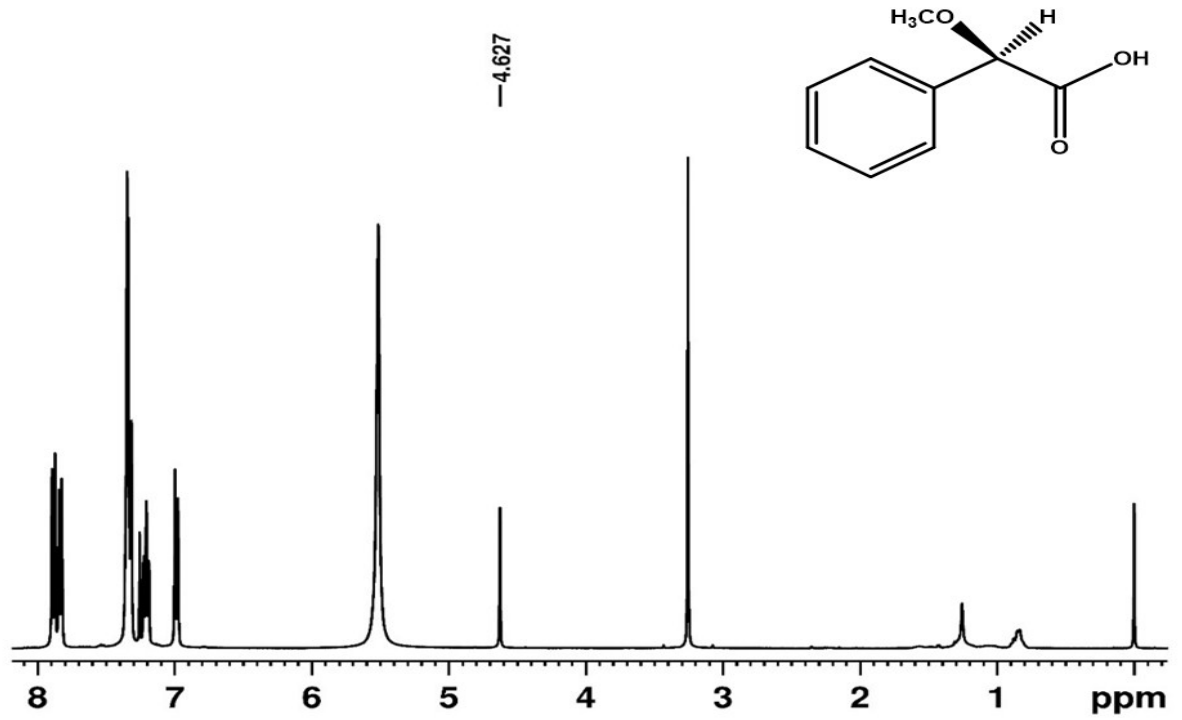

Fig. S21: 400 MHz ^{1}H-NMR spectrum of (*R*)-BINAM, (*R*)-(-)-α-methoxyphenylacetic acid and TFMS in $CDCl_3$

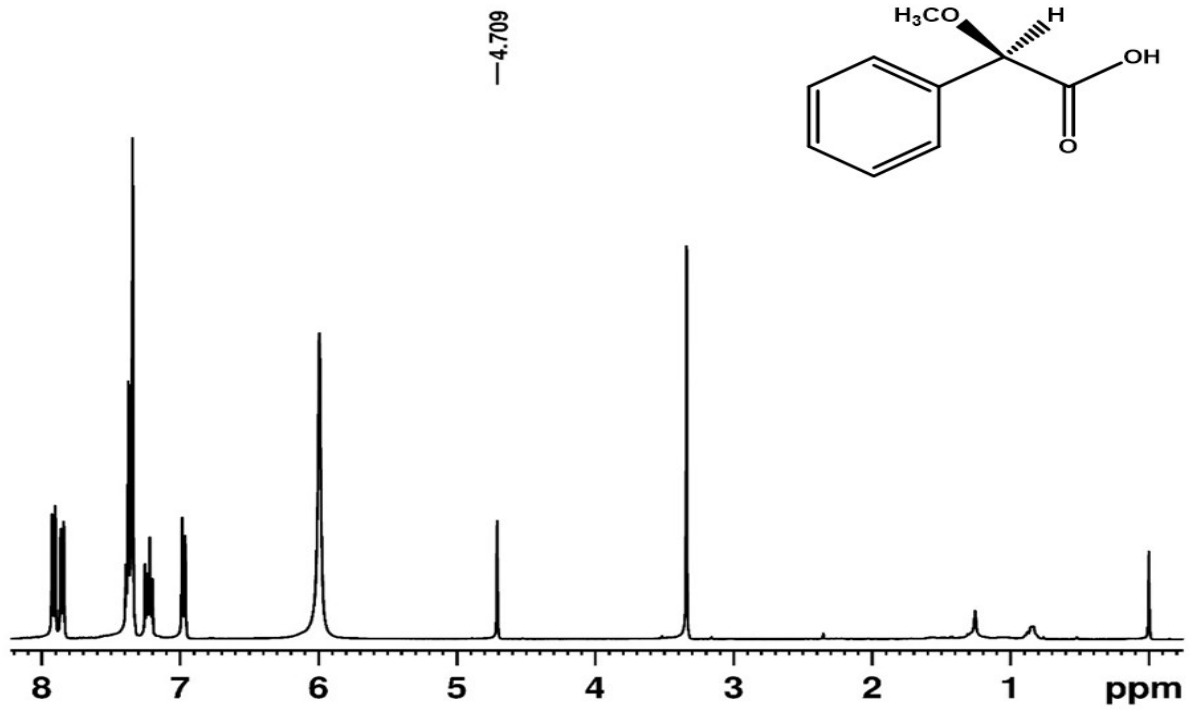

Fig. S22: 400 MHz ^{1}H-NMR spectrum of (*S*)-BINAM, (*R*)-(-)-α-methoxyphenylacetic acid and TFMS in $CDCl_3$

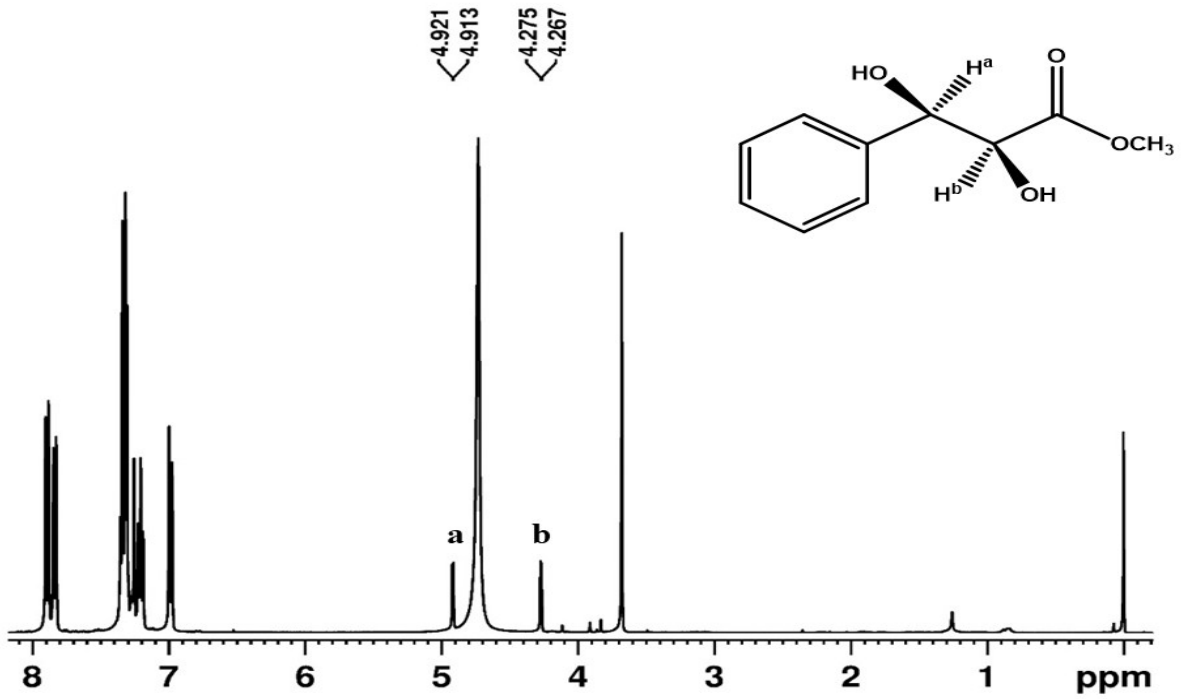

Fig. S23: 400 MHz ^{1}H-NMR spectrum of (*R*)-BINAM, Methyl (2*S*,3*R*)-(-)-2,3-dihydroxy-3-phenylpropionate and TFMS in $CDCl_3$

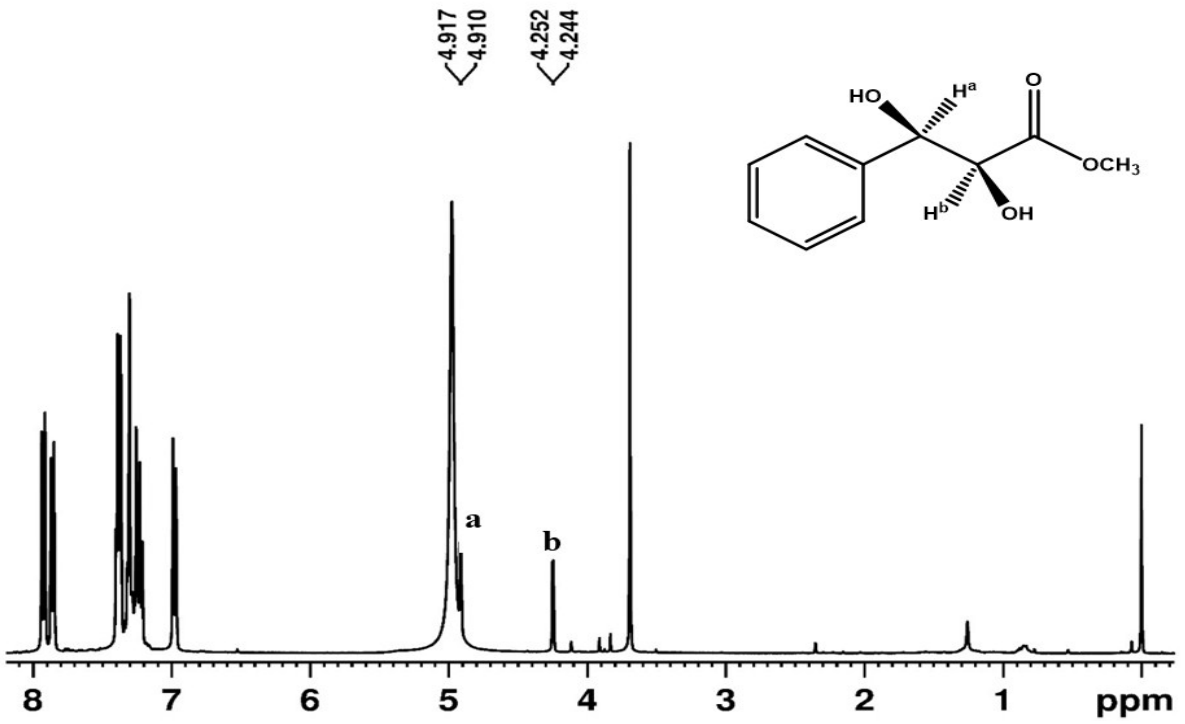

Fig. S24: 400 MHz ^{1}H-NMR spectrum of (*S*)-BINAM, Methyl (2*S*,3*R*)-(-)-2,3-dihydroxy-3-phenylpropionate and TFMS in $CDCl_3$

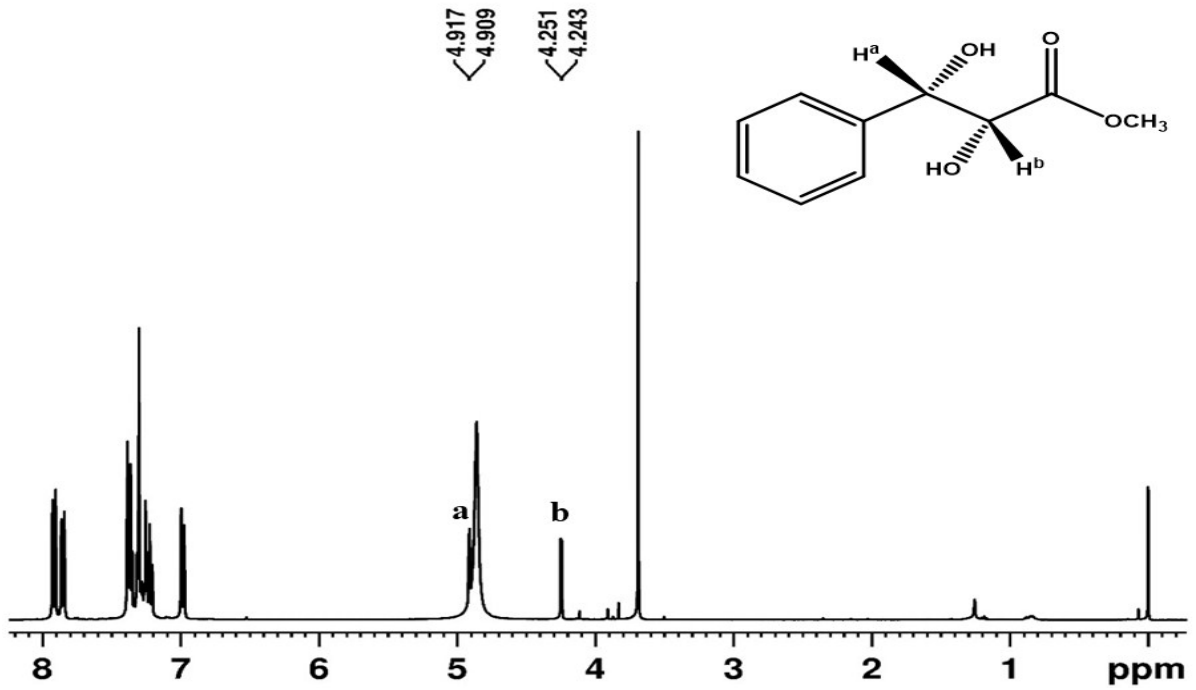

Fig. S25: 400 MHz ^{1}H-NMR spectrum of (*R*)-BINAM, Methyl (2*R*,3*S*)-(+)-2,3-dihydroxy-3-phenylpropionate and TFMS in $CDCl_3$

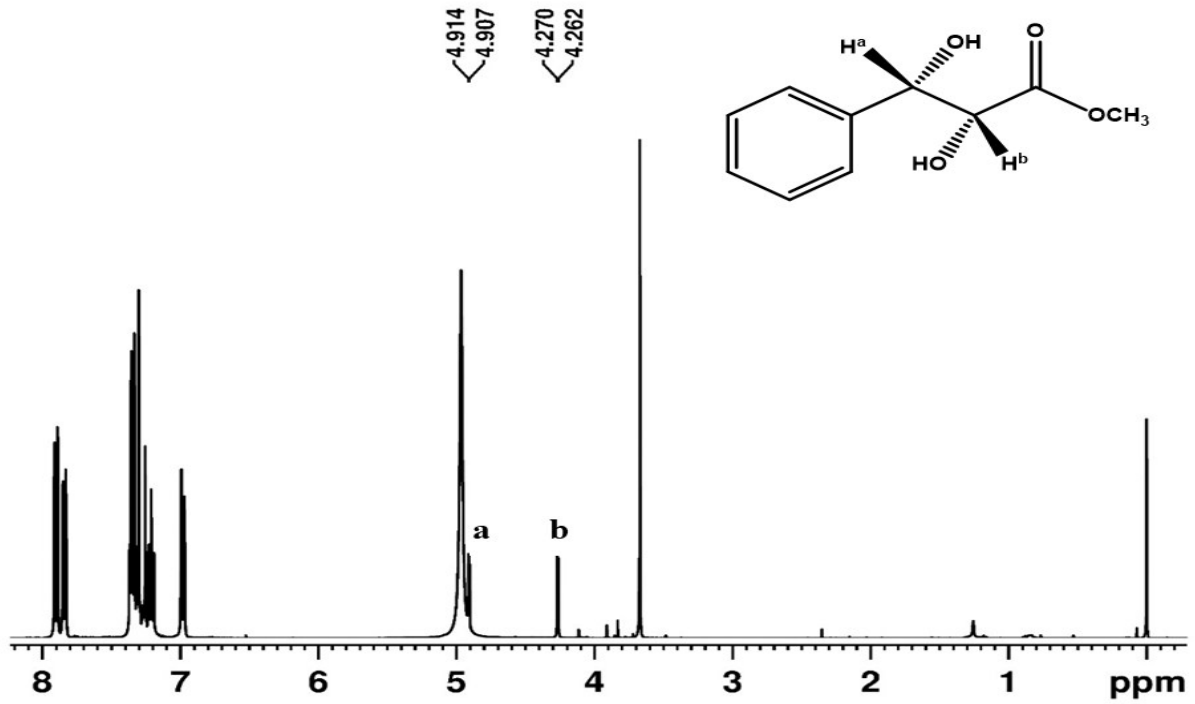

Fig. S26: 400 MHz ^{1}H-NMR spectrum of (*S*)-BINAM, Methyl (2*R*,3*S*)-(+)-2,3-dihydroxy-3-phenylpropionate and TFMS in $CDCl_3$

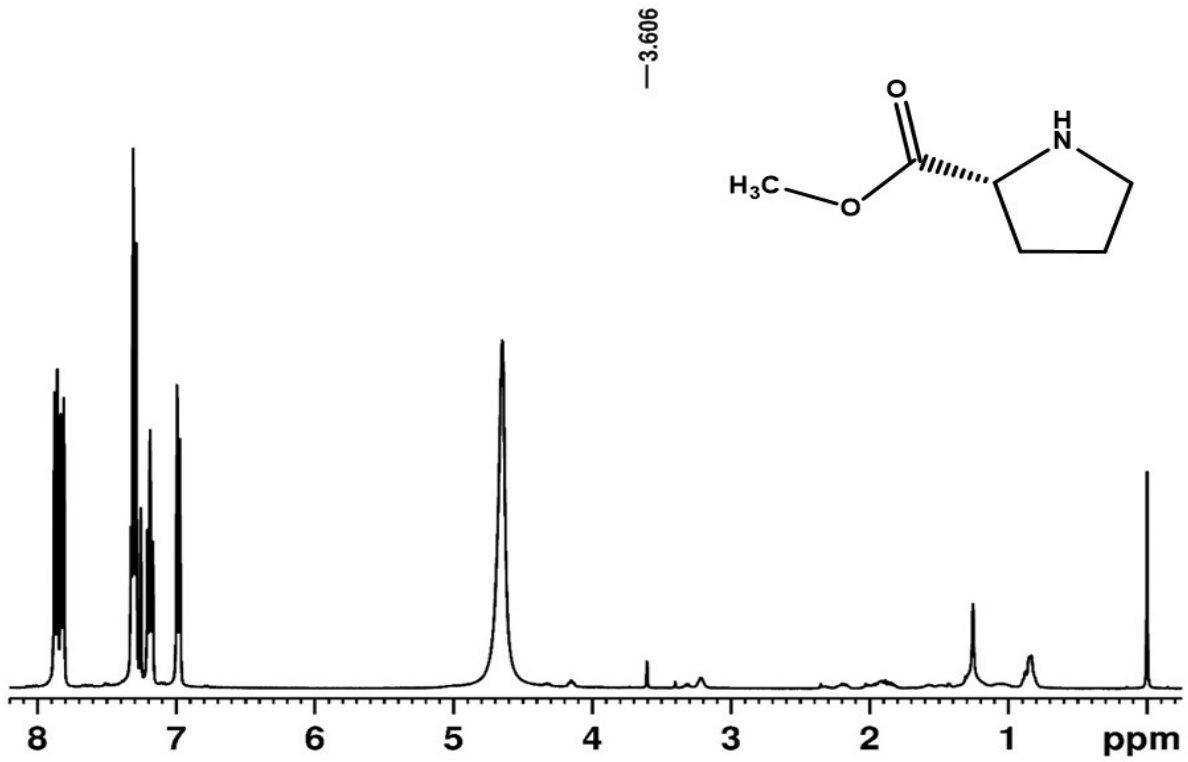

Fig. S27: 400 MHz ^{1}H-NMR spectrum of (*R*)-BINAM, (*R*)-pyrrolidine-2-carboxylic acid methyl ester and TFMS in $CDCl_3$

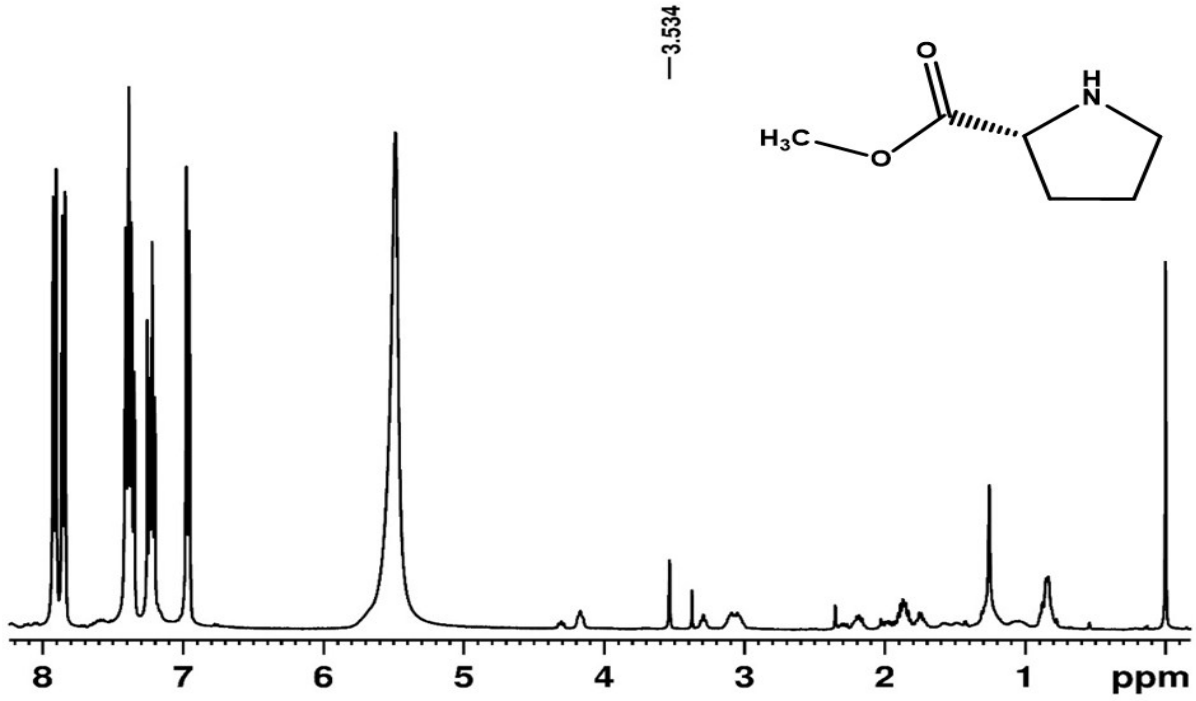

Fig. S28: 400 MHz ^{1}H-NMR spectrum of (*S*)-BINAM, (*R*)-pyrrolidine-2-carboxylic acid methyl ester and TFMS in $CDCl_3$

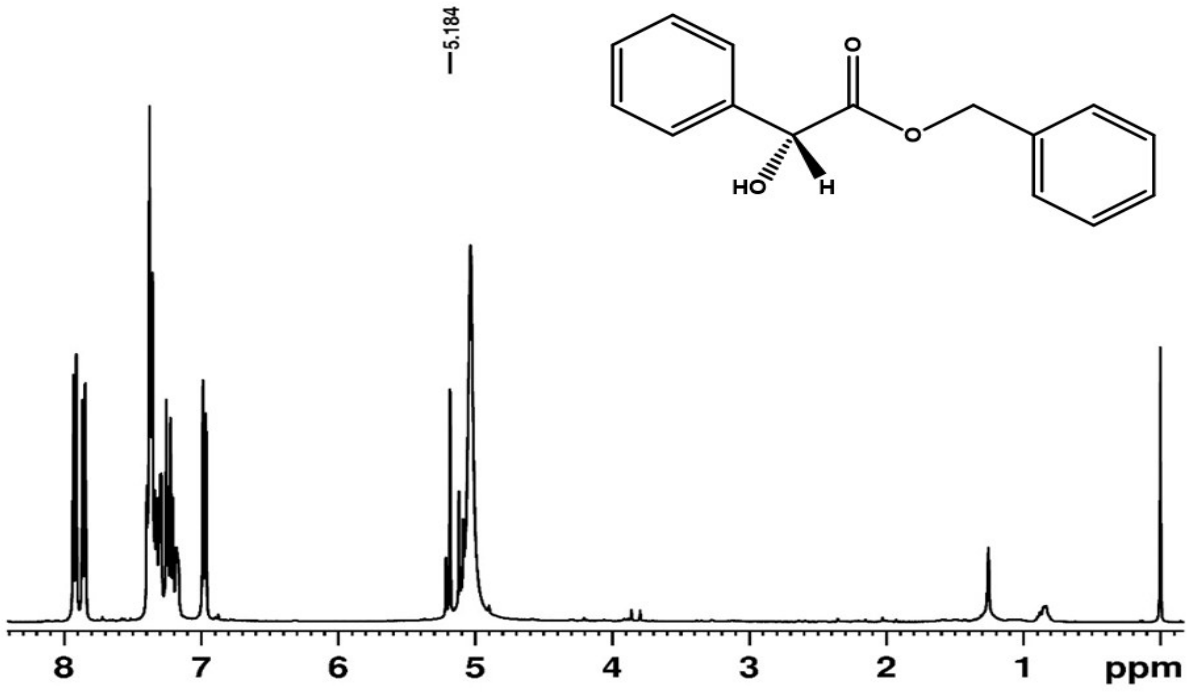

Fig. S29: 400 MHz ^{1}H-NMR spectrum of (*R*)-BINAM, Benzyl (*R*)-(-)-mandelate and TFMS in $CDCl_3$

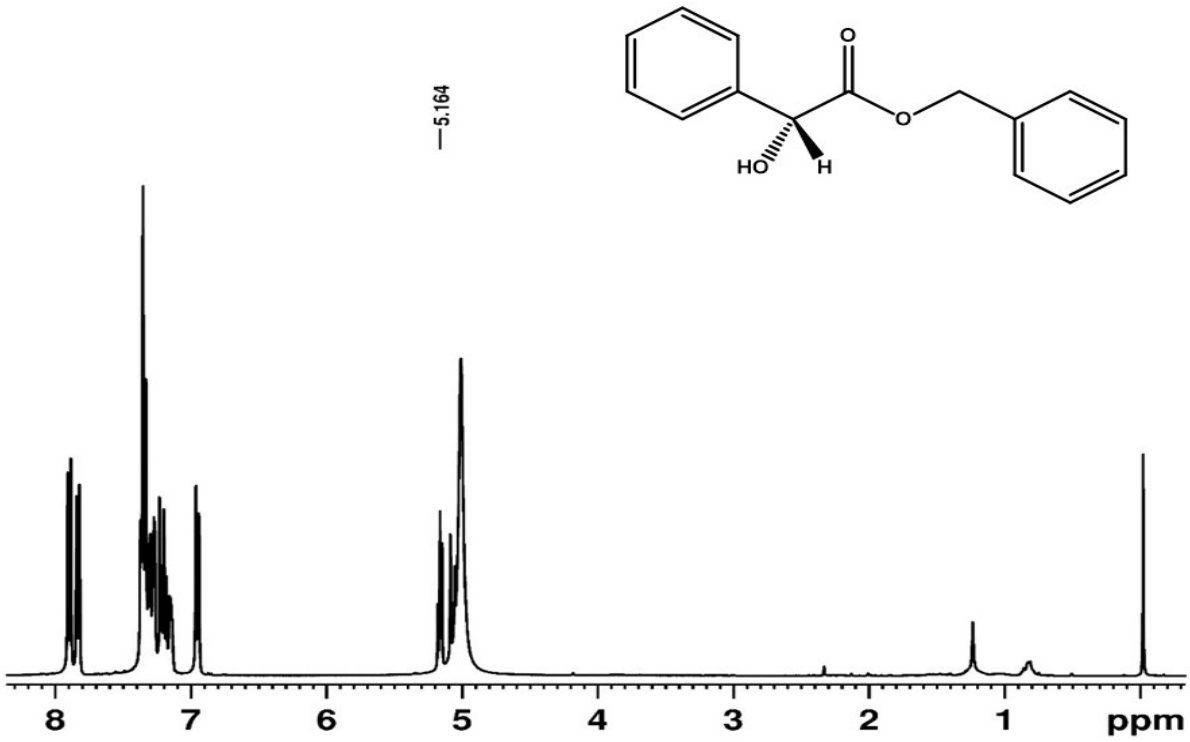

Fig. S30: 400 MHz ^{1}H-NMR spectrum of (*S*)-BINAM, Benzyl (*R*)-(-)-mandelate and TFMS in $CDCl_3$

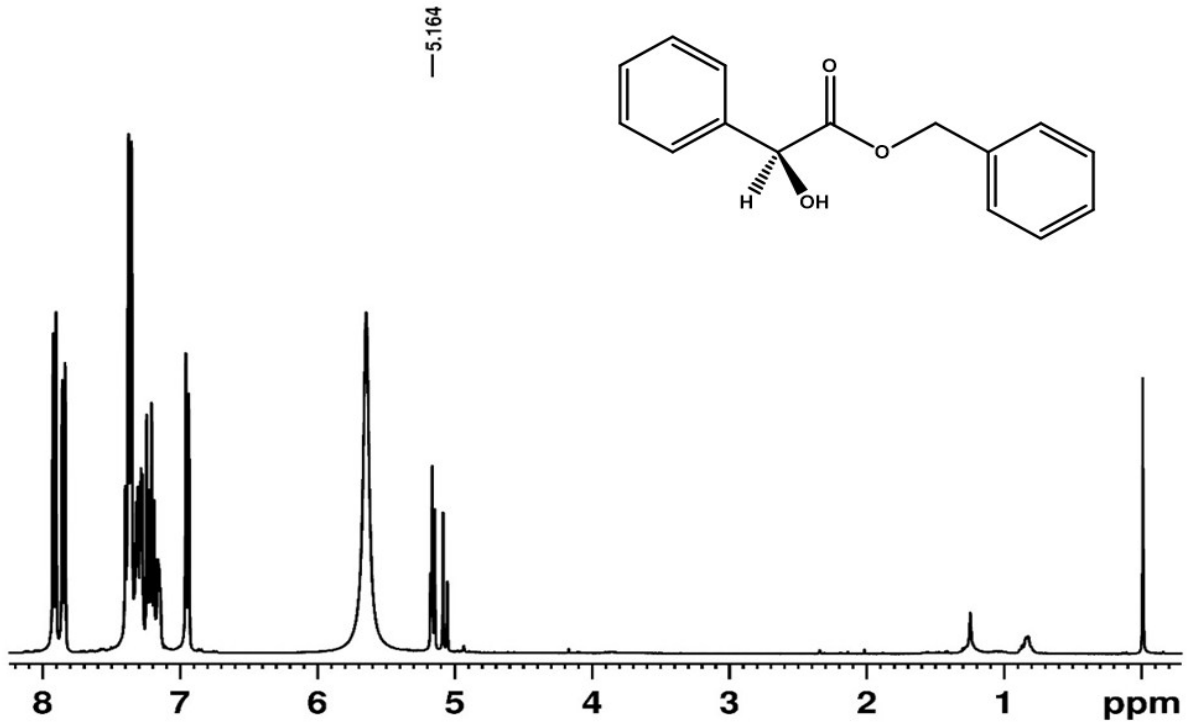

Fig. S31: 400 MHz ^{1}H-NMR spectrum of (*R*)-BINAM, Benzyl (*S*)-(+)-mandelate and TFMS in $CDCl_3$

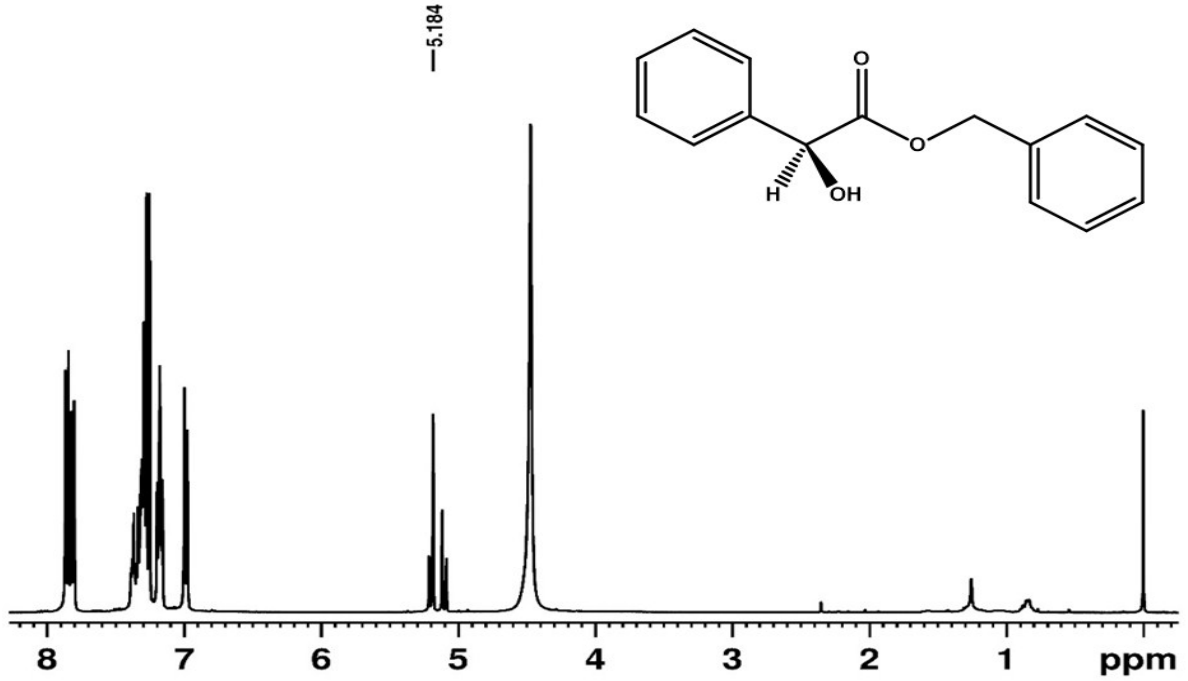

Fig. S32: 400 MHz ^{1}H-NMR spectrum of (*S*)-BINAM, Benzyl (*S*)-(+)-mandelate and TFMS in $CDCl_3$

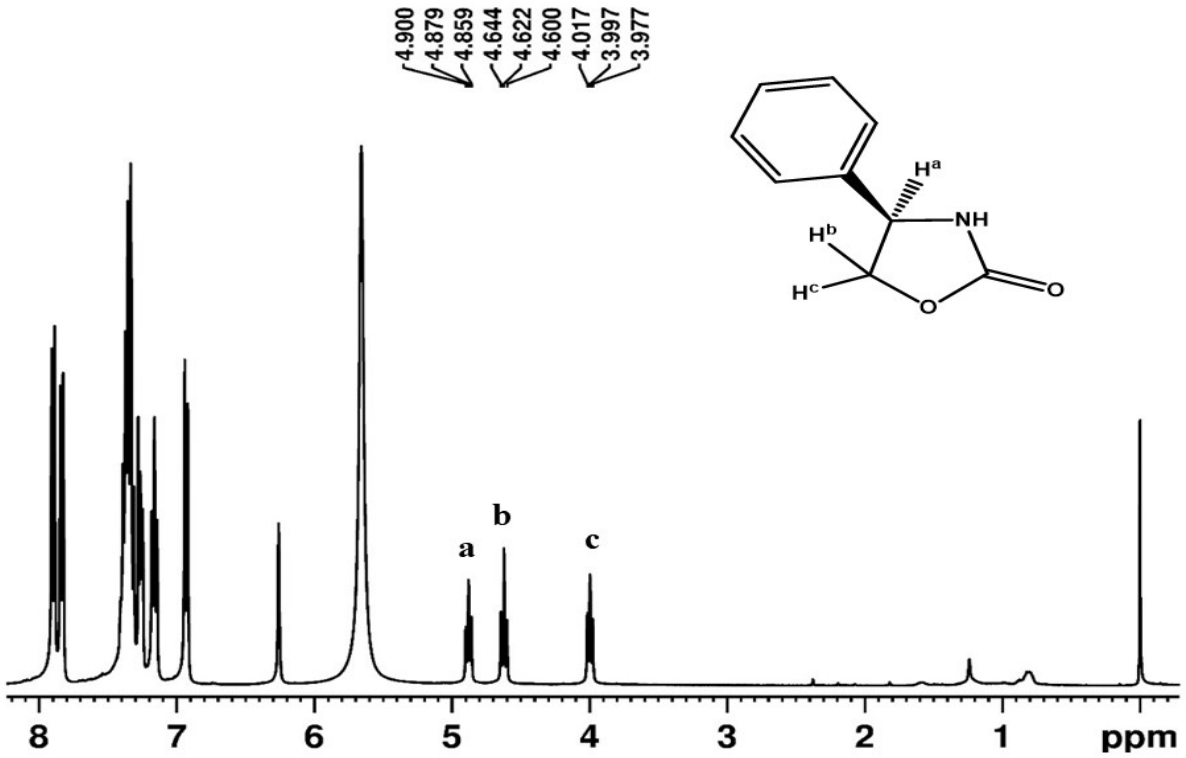

Fig. S33: 400 MHz ^{1}H-NMR spectrum of (*R*)-BINAM, (*R*)-(-)-4-phenyl-2-oxazolidione and TFMS in $CDCl_3$

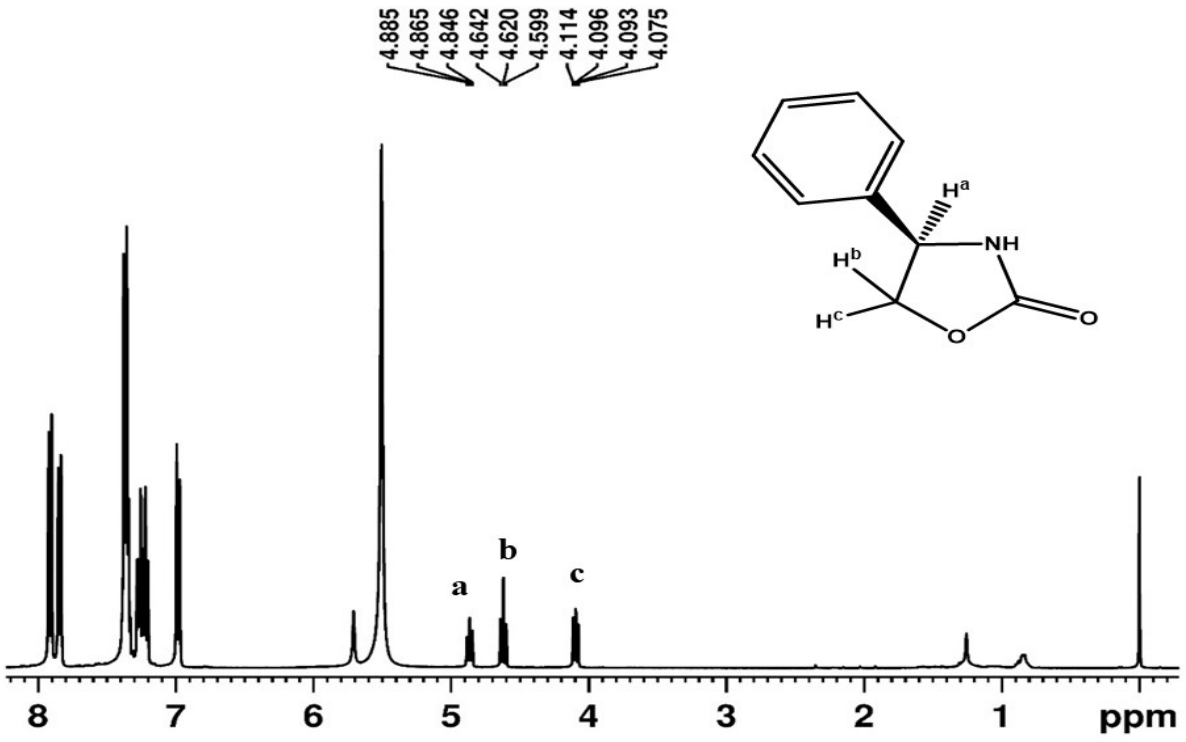

Fig. S34: S30400 MHz ^{1}H-NMR spectrum of (*S*)-BINAM, (*R*)-(-)-4-phenyl-2-oxazolidinone and TFMS in $CDCl_3$

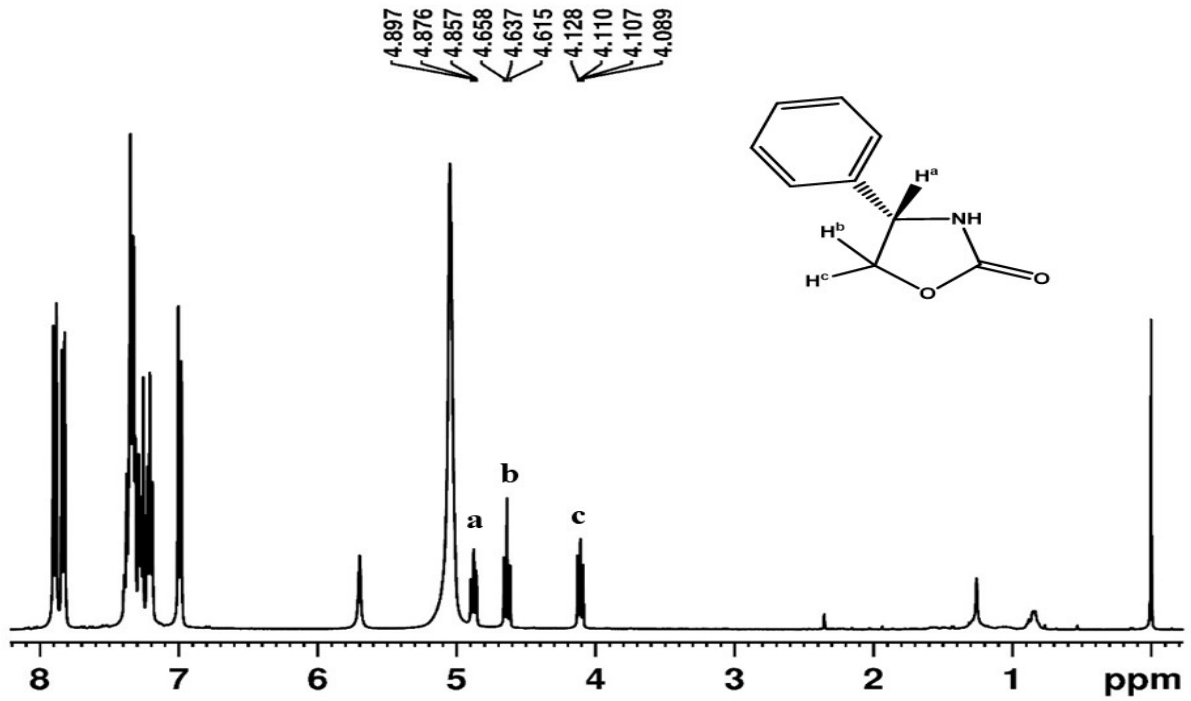

Fig. S35: 400 MHz ^{1}H-NMR spectrum of (*R*)-BINAM, (*S*)-(+)-4-phenyl-2-oxazolidinone and TFMS in $CDCl_3$

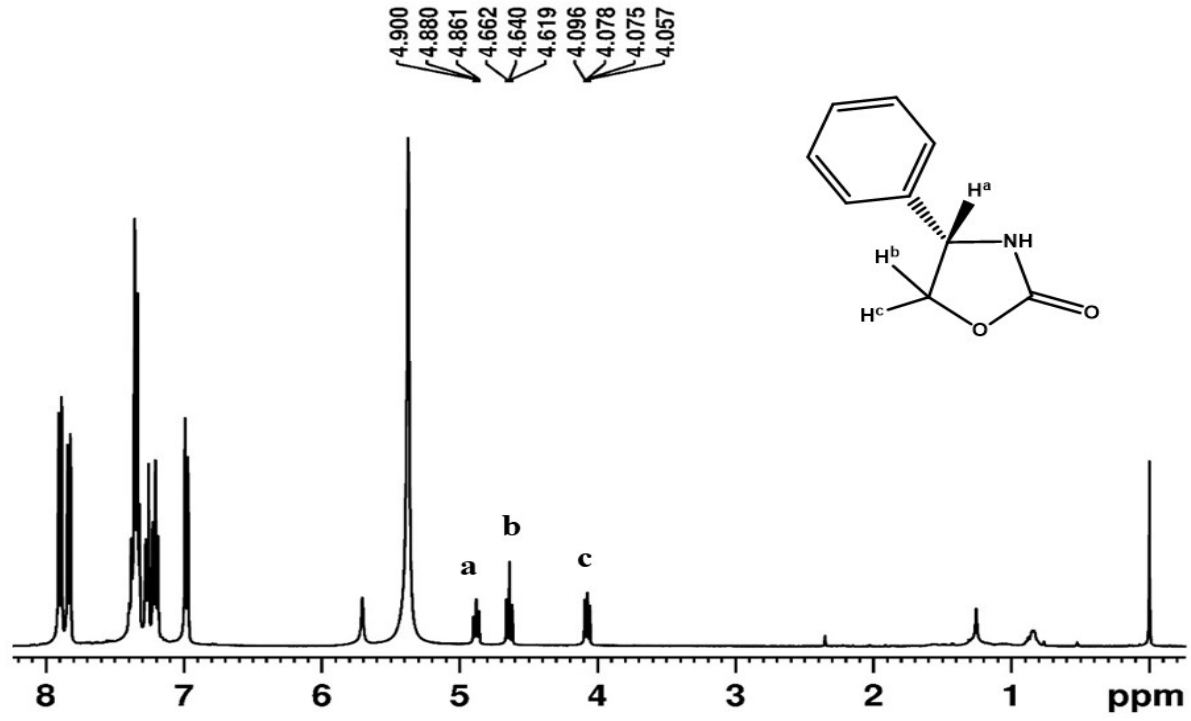

Fig. S36: 400 MHz ^{1}H-NMR spectrum of (*S*)-BINAM, (*S*)-(+)-4-phenyl-2-oxazolidinone and TFMS in $CDCl_3$

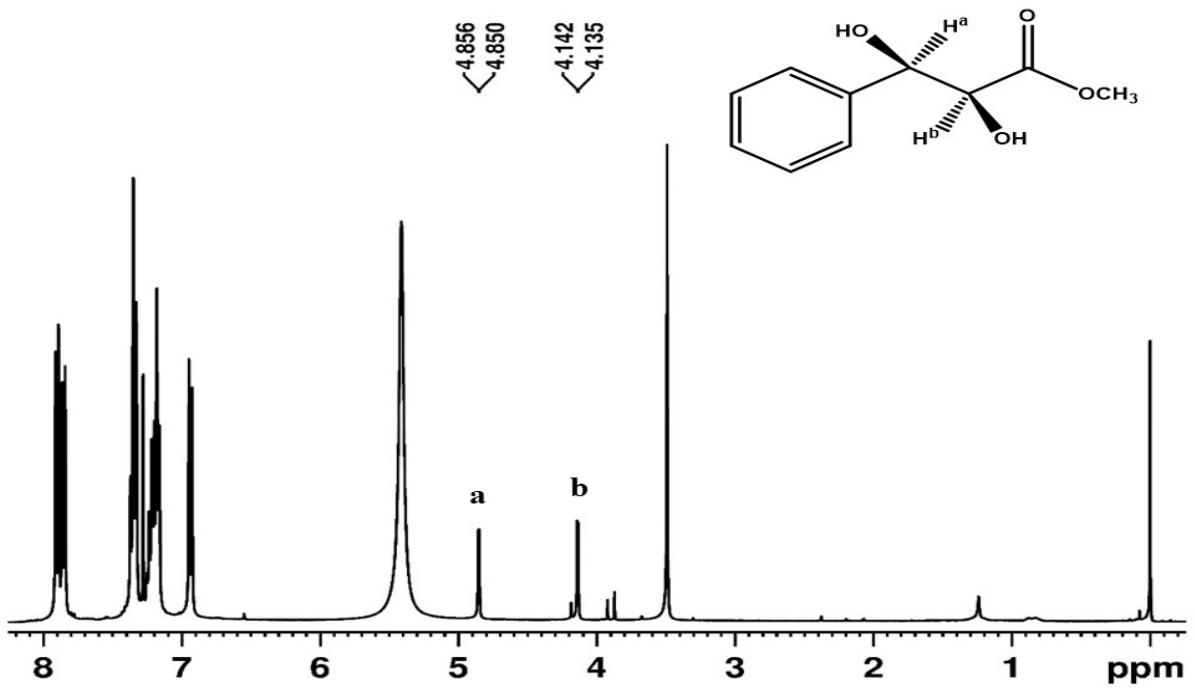

Fig. S37: 400 MHz ^{1}H-NMR spectrum of (*R*)-BINAM, Methyl (2*S*,3*R*)-(-)-2,3-dihydroxy-3-phenylpropionate and TFMS in $CDCl_3$ at 250K

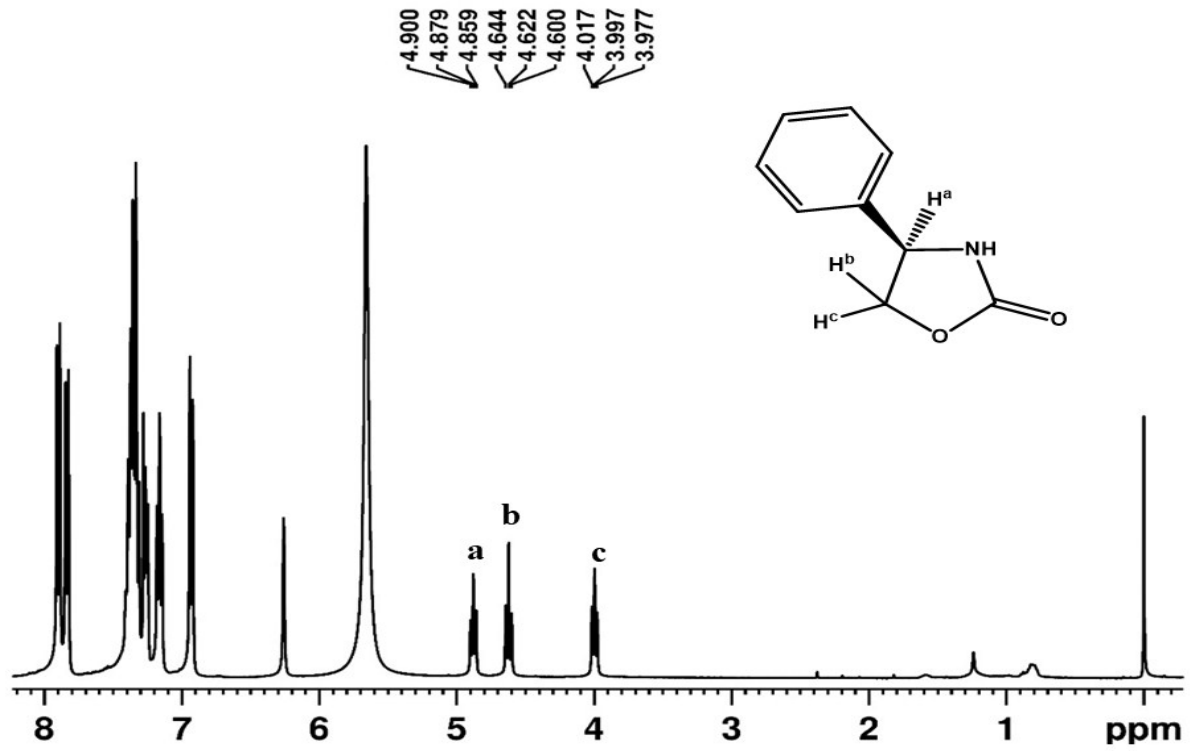

Fig. S38: 400 MHz ^{1}H-NMR spectrum of (*R*)-BINAM, (*R*)-(-)-4-phenyl-2-oxazolidinone and TFMS in $CDCl_3$ at 250K

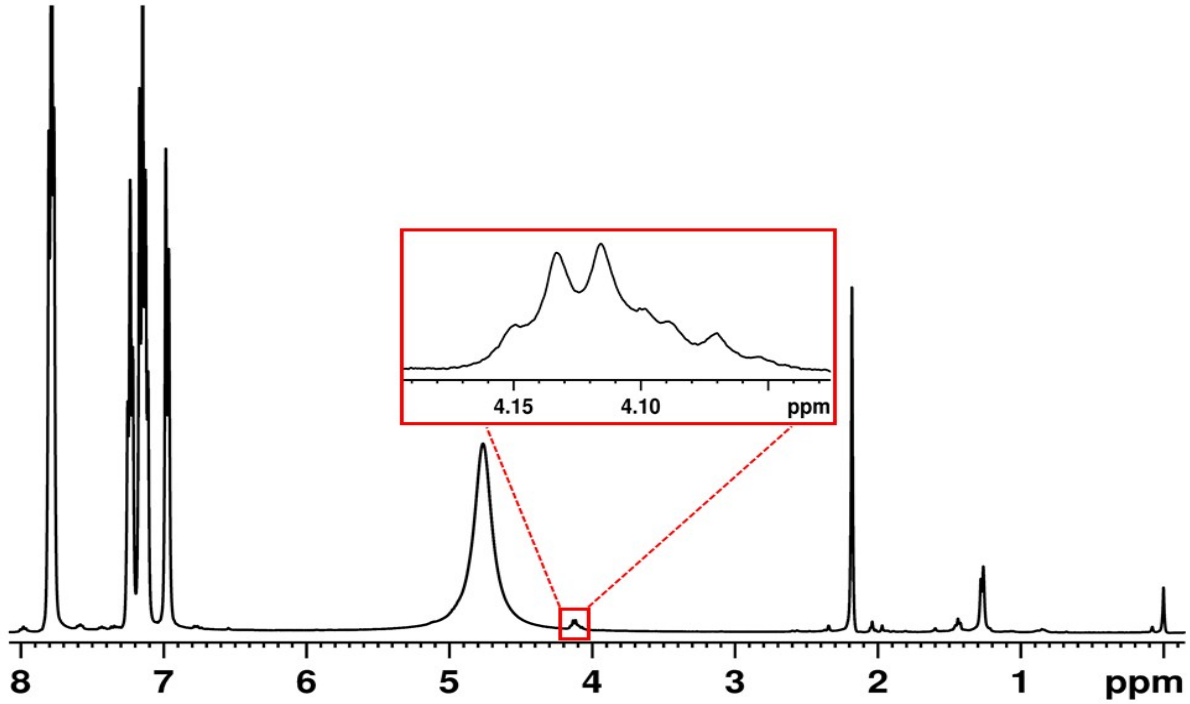

Fig. S39: 400 MHz ^{1}H-NMR spectrum of (*R*)-BINAM, Lactic acid (from deamination reaction of Alanine), and TFMS in $CDCl_3$ at 298K (RT) with zoomed α-proton region.

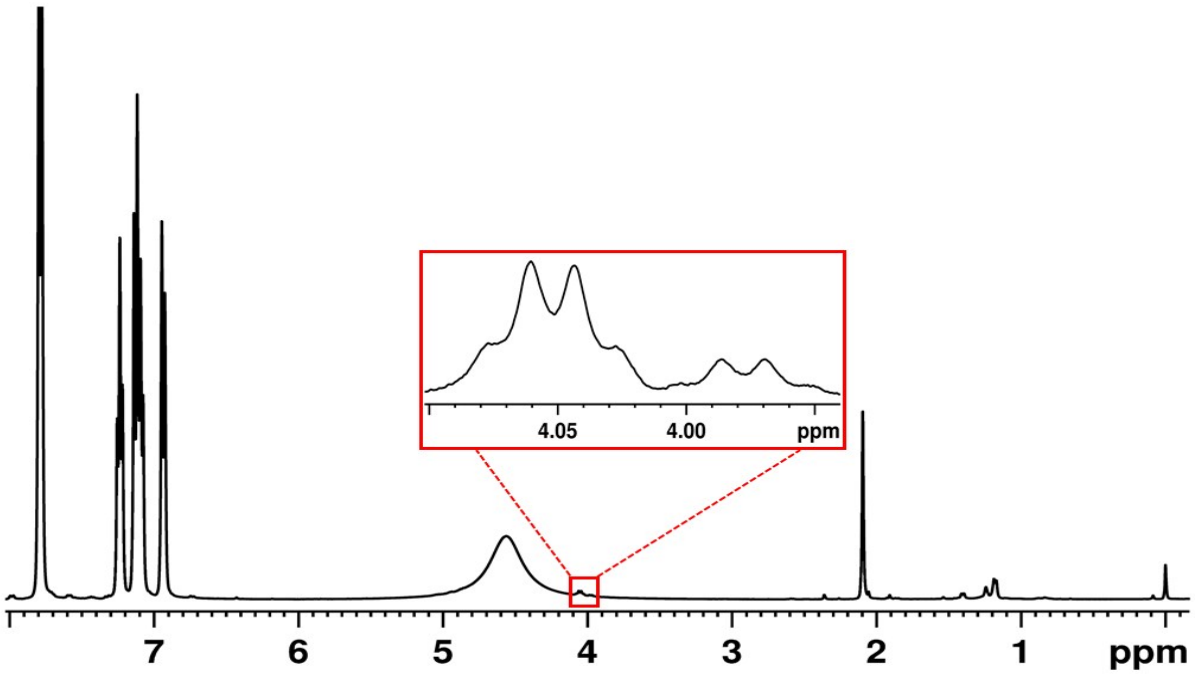

Fig. S40: 400 MHz ^{1}H-NMR spectrum of (*R*)-BINAM, Lactic acid (from deamination reaction of Alanine), and TFMS in $CDCl_3$ at 250K with zoomed α-proton region.

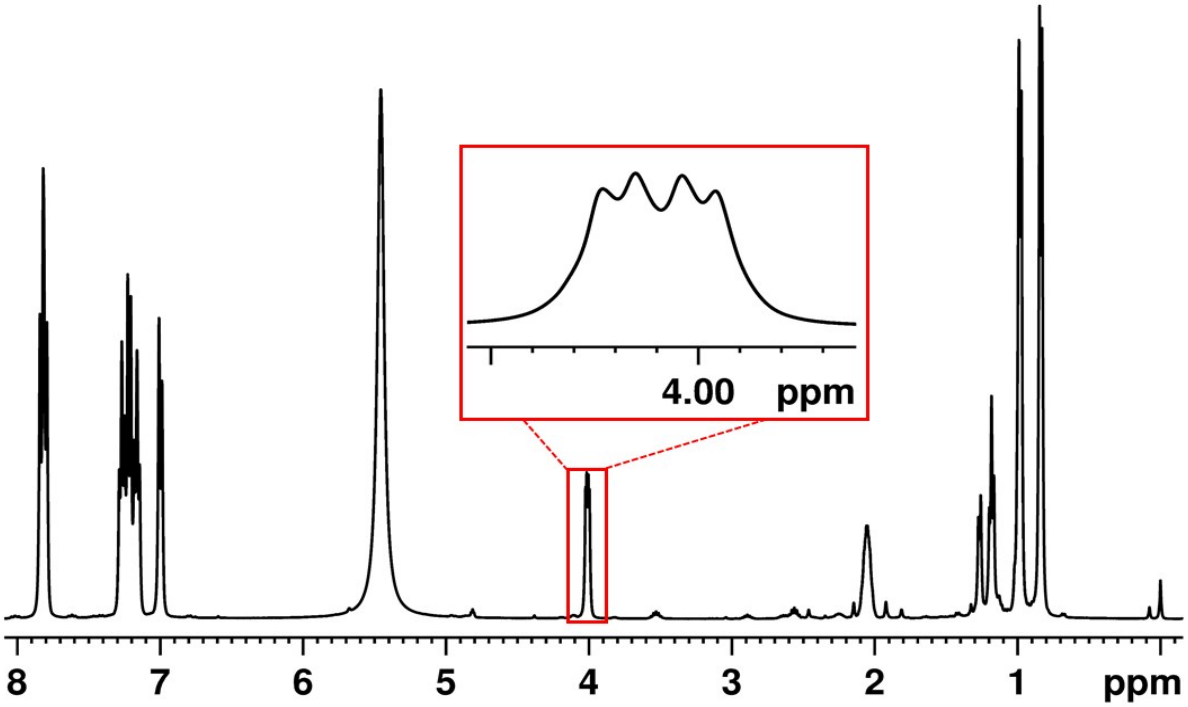

Fig. S41: 400 MHz ^{1}H-NMR spectrum of (*R*)-BINAM, 2-hydroxy-3-methylbutyric acid (from deamination reaction of Valine), and TFMS in $CDCl_3$ at 298K (RT) with zoomed α-proton region.

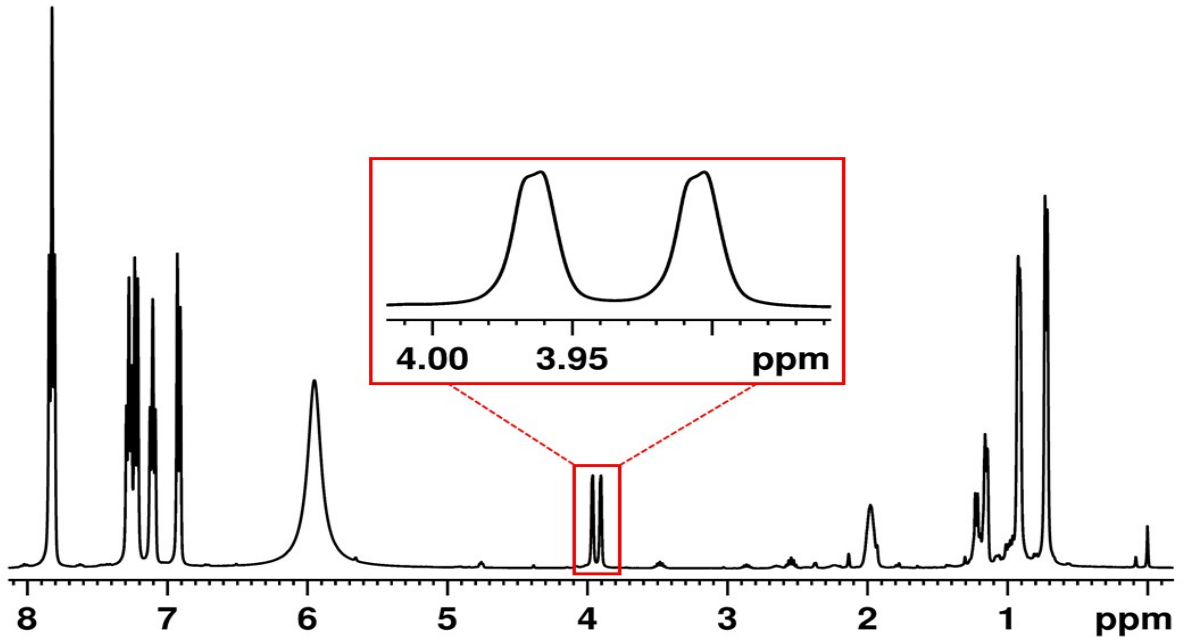

Fig. S42: 400 MHz ^{1}H-NMR spectrum of (*R*)-BINAM, 2-hydroxy-3-methylbutyric acid (from deamination reaction of Valine), and TFMS in $CDCl_3$ at 250K with zoomed α-proton region.

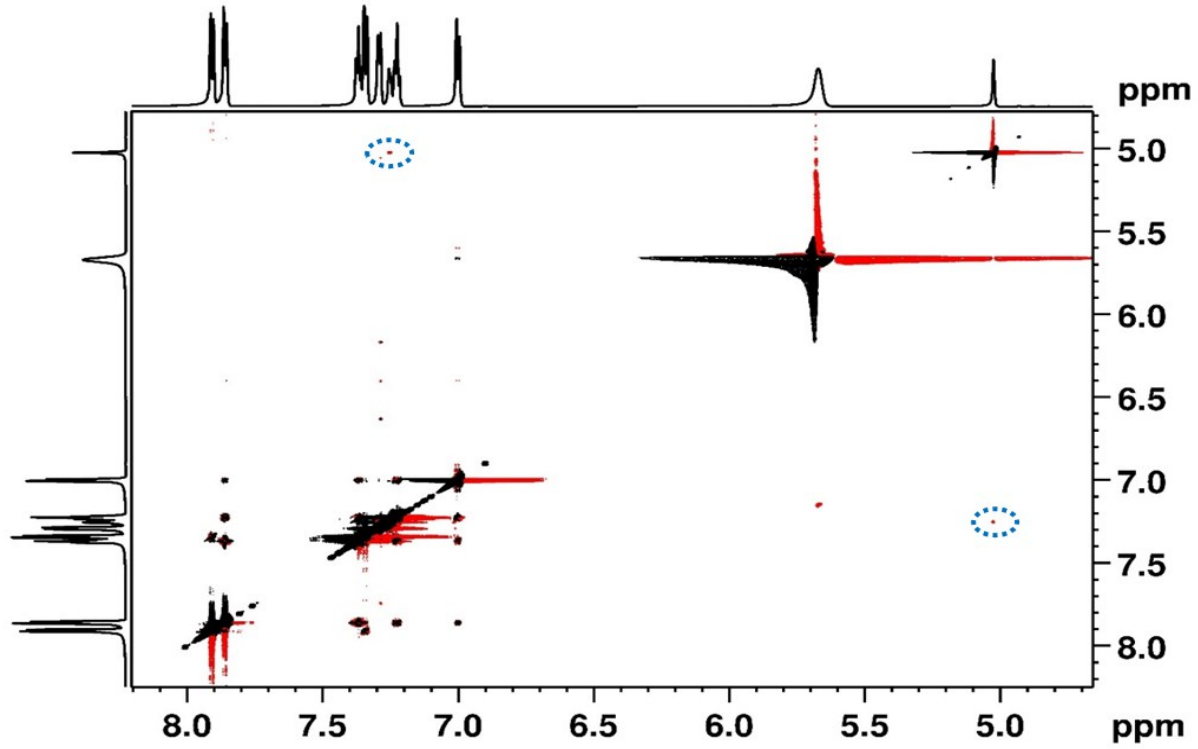

Fig. S43: 800 MHz 2D-NOSEY spectrum of (*R*)-BINAM, (*R*)-Mandelic acid and TFMS in $CDCl_3$

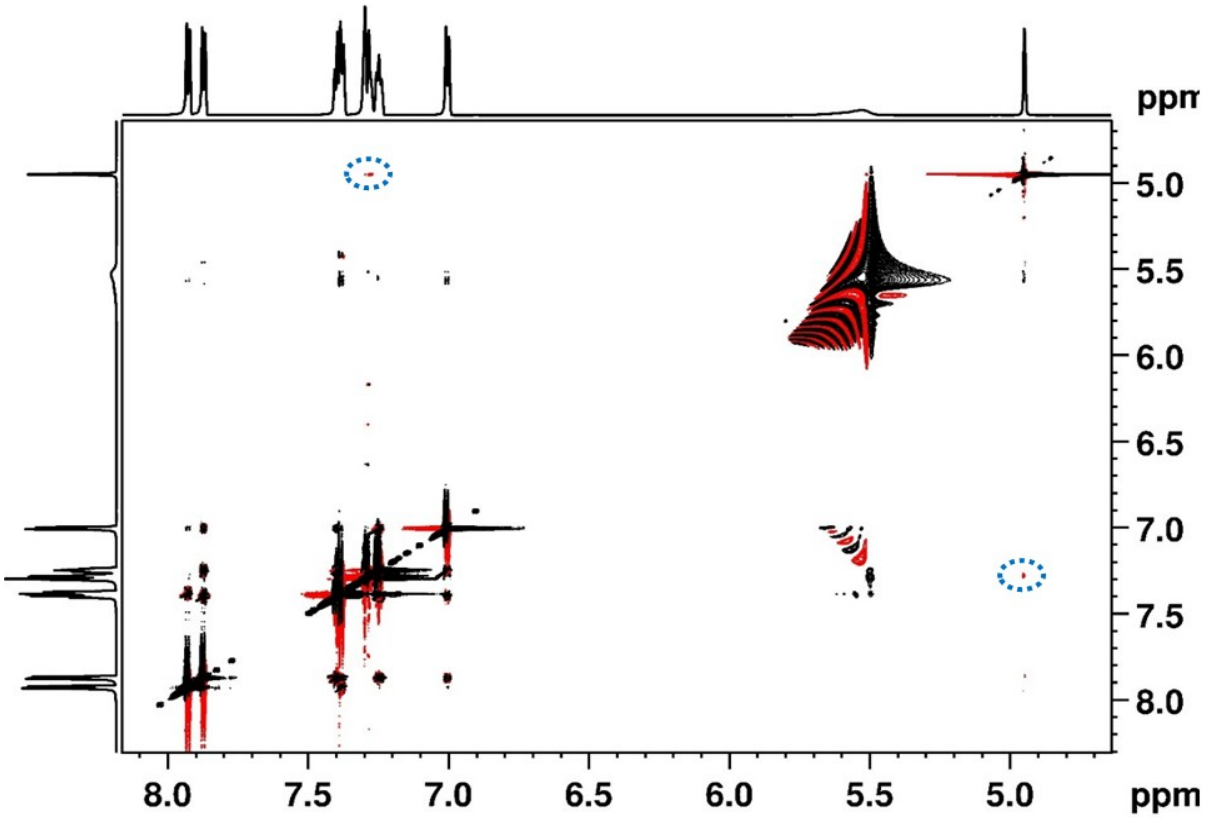

Fig. S44: 800 MHz 2D-NOSEY spectrum of (*S*)-BINAM, (*R*)-Mandelic acid and TFMS in $CDCl_3$

Table. S1: The experimentally determined and laboratory prepared scalemic ratios of (*R*)-BINAM and (*R/S*) – Mandelic acid in presence of TFMS

Entry	Integration I_R:I_S	Gravimetrically prepared excess of *S* enantiomer %	experimentally measured *ee* $ee\% = \frac{I_R - I_S}{I_R + I_S} \times 100$	% error
1	1.000:0.9987	0	0	0
2	1.000:0.8182	10	9.9	1.00
3	1.000:0.6616	20	20.3	1.50
4	1.000:0.5374	30	30.0	0
5	1.000:0.4290	40	39.9	0.25
6	1.000:0.3340	50	49.9	0.20
7	1.000:0.2502	60	59.9	0.16
8	1.000:0.1757	70	70.1	0.14
9	1.000:0.1113	80	79.9	0.13
10	1.000:0.0527	90	89.9	0.11
11	1.000:0.0206	96	95.9	0.10

Coordinates for (*R*)-BINAM/ (*R*)-Mandelic acid/ TFMS complex (Gaussian 09)

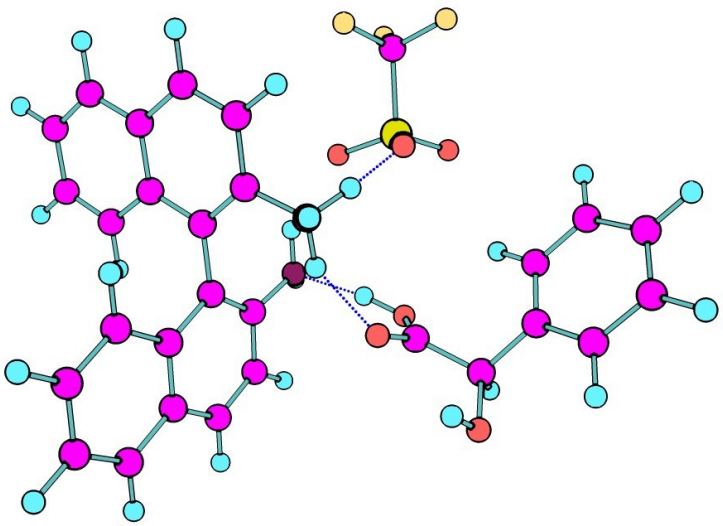

C	1.43774	0.62738	-1.38000
C	2.38915	0.21588	-0.46102
C	3.56448	1.02075	-0.24697
C	3.73778	2.22418	-1.00392
C	2.73935	2.59805	-1.94065
C	1.62213	1.82671	-2.11795
H	4.45138	-0.22192	1.29518
C	4.56515	0.68014	0.70477
C	4.89274	3.02194	-0.79275
H	2.86543	3.51736	-2.50554
H	0.83987	2.13637	-2.80278
C	5.84430	2.65962	0.13255
C	5.67329	1.47781	0.88892
H	5.00684	3.93192	-1.37557
H	6.72234	3.27920	0.28736
H	6.42223	1.19641	1.62332

C	2.22658	-1.04855	0.32234
C	2.99397	-2.21684	-0.02170
C	1.38706	-1.13100	1.41589
C	3.85708	-2.24080	-1.15126
C	2.89055	-3.40138	0.77840
C	1.27406	-2.29864	2.20738
C	4.57908	-3.37010	-1.46691
H	3.94128	-1.35326	-1.76751
C	3.65253	-4.54738	0.42802
C	2.02095	-3.40626	1.90011
H	0.57898	-2.31274	3.04113
C	4.48035	-4.53463	-0.67042
H	5.23025	-3.36743	-2.33573
H	3.56464	-5.43817	1.04383
H	1.94050	-4.30476	2.50449
H	5.05657	-5.41724	-0.93060
N	0.21652	-0.12699	-1.58910
N	0.48175	-0.03070	1.77542
H	0.28462	-0.64124	-2.44403
H	0.57980	0.23533	2.75750
S	-1.42029	2.40178	0.29910
O	-1.57198	2.15909	-1.15755
O	-2.31264	1.62063	1.18001
O	0.00981	2.40141	0.76198
C	-1.92652	4.17689	0.52107
F	-3.20958	4.33402	0.17260
F	-1.17294	4.97835	-0.24197
F	-1.78187	4.54407	1.80092
C	-2.10908	-1.93035	0.65416
O	-1.77378	-1.32182	1.66657

O	-1.48163	-1.89115	-0.50603
C	-3.35412	-2.81574	0.62218
C	-4.56887	-2.01401	0.13591
C	-5.56805	-2.68007	-0.58309
C	-4.71449	-0.64851	0.41504
C	-6.69946	-1.99090	-1.02046
H	-5.45119	-3.73766	-0.79450
C	-5.84629	0.03629	-0.02968
H	-3.95233	-0.10196	0.96253
C	-6.84122	-0.62999	-0.74617
H	-7.46889	-2.51897	-1.57688
H	-5.93902	1.09722	0.18175
H	-7.71949	-0.09189	-1.09118
O	-3.11958	-3.99020	-0.13456
H	-2.87045	-3.70132	-1.02507
H	-3.52112	-3.15192	1.65055
H	0.53464	0.87452	1.22383
H	-0.97197	-0.82428	1.49008
H	0.08236	-0.76171	-0.82809
H	-1.11760	1.34768	-1.39580

Coordinates BINAM/ Mandelic complex

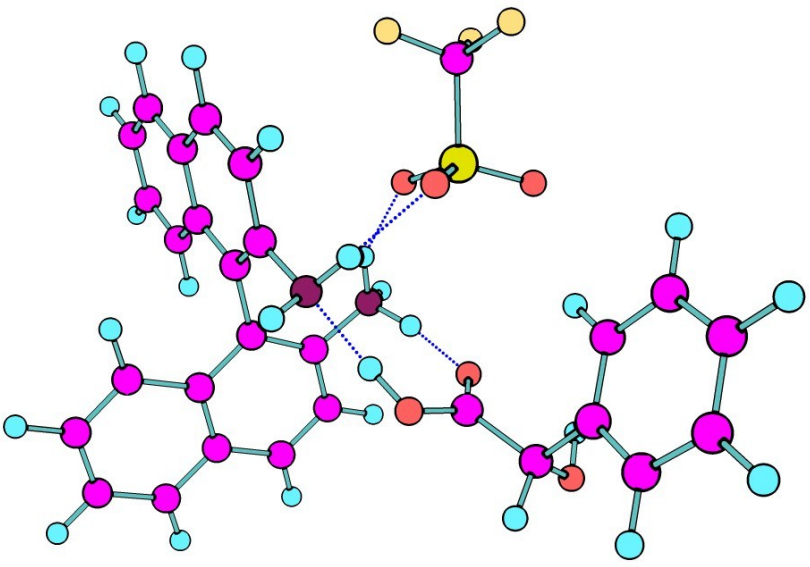

for (*R*)-(*S*)- acid/ TFMS

(Gaussian 09)

C	-0.86816	-1.03087	-1.74312
C	-0.09755	-0.15921	-0.95563
C	1.21045	0.22568	-1.40423
C	1.71813	-0.27245	-2.65572
C	0.89914	-1.15062	-3.42001
C	-0.34889	-1.52007	-2.98226
H	1.68210	1.47428	0.30280
C	2.04759	1.09898	-0.64634
C	3.01343	0.11759	-3.09343
H	1.27796	-1.53078	-4.36478
H	-0.96177	-2.19271	-3.57630
C	3.79530	0.96714	-2.33590
C	3.30202	1.45797	-1.10010
H	3.37901	-0.26973	-4.04108
H	4.78314	1.25789	-2.67856
H	3.92035	2.12155	-0.50301
C	-0.65927	0.36162	0.33379

C	-0.56077	-0.39917	1.54697
C	-1.30176	1.61086	0.35317
C	0.08833	-1.66960	1.59699
C	-1.12629	0.11439	2.76703
C	-1.85553	2.10927	1.57354
C	0.16804	-2.38514	2.77599
H	0.52729	-2.06449	0.68778
C	-1.02705	-0.64834	3.96282
C	-1.77011	1.38348	2.73614
H	-2.34881	3.07755	1.56628
C	-0.39456	-1.87583	3.97412
H	0.66989	-3.34804	2.78781
H	-1.46008	-0.24305	4.87383
H	-2.19743	1.77662	3.65455
H	-0.32330	-2.44963	4.89253
N	-2.12997	-1.42711	-1.34674
H	-2.55121	-0.70208	-0.80186
H	-2.69199	-1.60660	-2.15416
N	-1.41609	2.37477	-0.79124
H	-1.46124	1.77436	-1.58966
H	-2.24847	2.92676	-0.74177
H	-2.06061	-2.25963	-0.79710
H	-0.62137	2.97646	-0.87115
S	-2.54465	1.19589	-3.67664
O	-2.32446	-0.36120	-3.11463
O	-4.02201	1.48005	-3.80619
O	-1.86190	2.27715	-2.60257
C	-1.90562	1.33716	-4.98174
F	-2.57861	0.60413	-5.89402
F	-0.62977	0.90218	-4.90752

F	-1.91758	2.63578	-5.35045
C	-3.73760	0.68322	-0.86892
O	-3.16718	1.61512	-1.57571
O	-3.57696	-0.56747	-1.19037
C	-4.60278	1.06049	0.34794
C	-5.14932	-0.10082	0.91059
C	-5.99857	-0.00844	2.01364
C	-4.84438	-1.34900	0.36782
C	-6.54218	-1.16410	2.57414
H	-6.23816	0.97569	2.44179
C	-5.38886	-2.50503	0.92777
H	-4.17520	-1.42197	-0.50166
C	-6.23754	-2.41280	2.03084
H	-7.21108	-1.09142	3.44396
H	-5.14859	-3.48901	0.49936
H	-6.66633	-3.32385	2.47292
O	-5.65833	1.93046	-0.06903
H	-6.14165	1.52418	-0.79217
H	-4.05133	1.51355	1.01031

Coordinates for (*S*)-BINAM/ (*R*)-Mandelic acid/ TFMS complex (Gaussian 09)

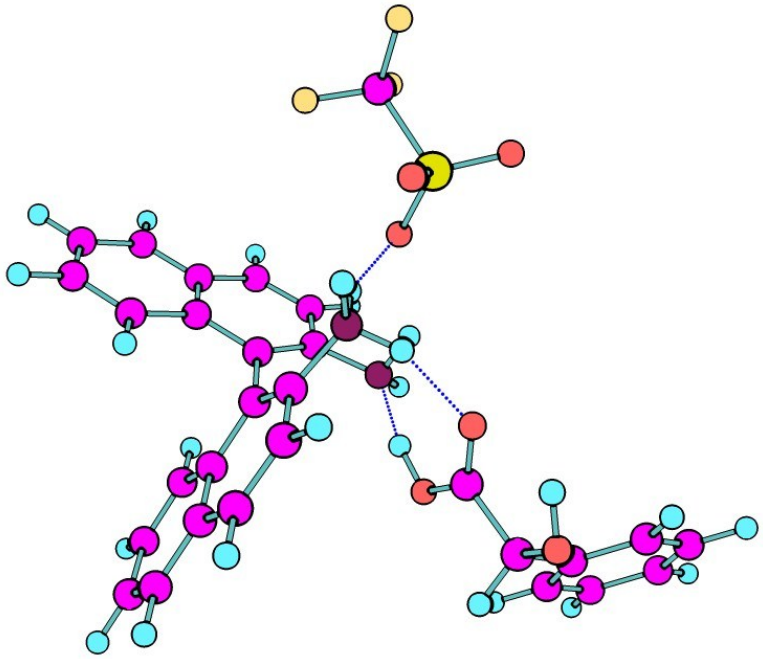

C	2.28979	-1.00965	0.32991
C	1.26851	-1.39119	-0.59852
C	0.87806	-2.75183	-0.68613
C	1.45482	-3.70748	0.11617
C	2.44959	-3.33217	1.04633
C	2.85688	-2.02200	1.15128
C	2.67664	0.36667	0.41722
H	0.10790	-3.02430	-1.39994
H	1.14797	-4.74420	0.04190
H	2.89721	-4.08564	1.68467
H	3.62101	-1.75507	1.87058
C	0.65930	-0.39107	-1.40098
C	1.02837	0.92259	-1.29787
C	2.04289	1.30728	-0.38408
C	3.73661	0.82999	1.36182

H	-0.11681	-0.68158	-2.10041
H	0.55611	1.68502	-1.90635
C	5.12299	0.53624	1.13751
C	6.10634	0.99804	2.07090
C	5.69619	1.75767	3.19531
C	4.37370	2.05868	3.38808
C	3.41632	1.58868	2.46750
C	5.56333	-0.18487	-0.00432
C	6.89732	-0.45115	-0.19959
C	7.86371	-0.01235	0.73401
C	7.47513	0.69849	1.84236
H	6.44233	2.10720	3.89929
H	4.06050	2.65244	4.23944
N	2.01555	1.96862	2.71255
H	4.83283	-0.52005	-0.72864
H	7.21333	-0.99934	-1.07956
H	8.91168	-0.23252	0.56693
H	8.21047	1.04915	2.55819
S	-1.03307	2.56490	1.62629
O	-0.90627	1.76852	2.86703
O	-0.00759	2.27707	0.60097
O	-1.28486	4.00830	1.85428
C	2.62855	7.87206	1.31926
C	3.17573	8.37476	0.13604
C	2.44182	9.24748	-0.66377
C	1.15484	9.62877	-0.28579
C	0.60819	9.13286	0.89641
C	1.34119	8.25759	1.69615
C	3.42737	6.90926	2.19661
H	4.17694	8.08327	-0.16161
H	2.87767	9.63483	-1.57779
H	0.58547	10.31232	-0.90541
H	-0.38903	9.43087	1.20075

H	0.92560	7.88573	2.62424
C	3.25341	5.46650	1.70741
H	4.49163	7.15001	2.10069
O	3.06437	6.98414	3.55808
O	3.77337	5.24597	0.52564
O	2.67760	4.63852	2.39836
H	2.58080	6.16807	3.75360
C	-2.63286	1.95074	0.87197
F	-2.54670	0.64404	0.61637
F	-3.64695	2.16250	1.71466
F	-2.87617	2.60058	-0.26861
N	2.42912	2.60252	-0.27134
H	1.92300	2.96206	2.64542
H	2.09524	2.97579	0.59422
H	2.04947	3.13088	-1.03075
H	1.42776	1.53229	2.03129
H	1.74424	1.66964	3.62743
H	3.42743	2.65588	-0.29436

Coordinates for (*S*)-BINAM/ (*S*)-Mandelic acid/ TFMS complex (Gaussian 09)

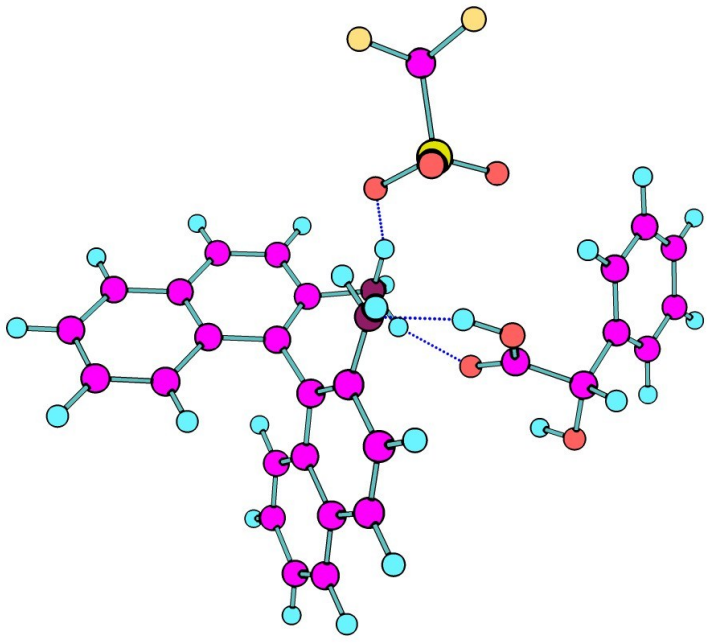

C	2.95062	-1.47687	0.75595
C	3.72712	-1.05236	1.88236
C	5.10352	-1.39226	1.95472
C	5.70721	-2.11371	0.95140
C	4.95046	-2.52185	-0.17025
C	3.61082	-2.21500	-0.26505
C	1.54998	-1.13375	0.68561
H	5.67414	-1.06052	2.81779
H	6.76195	-2.36313	1.01329
H	5.43076	-3.07953	-0.96860
H	3.05236	-2.53272	-1.13749
C	3.10289	-0.28702	2.90092
C	1.78744	0.07584	2.79079
C	1.00540	-0.33246	1.67943
C	0.73692	-1.69887	-0.44140
H	3.69068	0.03326	3.75635
H	1.32728	0.70461	3.54759
C	0.45669	-3.11333	-0.47131
C	-0.21839	-3.68348	-1.60040
C	-0.61559	-2.84183	-2.67200
C	-0.38768	-1.49165	-2.61666
C	0.28184	-0.93652	-1.50130
C	0.80976	-3.97596	0.60252
C	0.52434	-5.32229	0.55490
C	-0.12435	-5.88329	-0.56922
C	-0.48831	-5.07756	-1.62256
H	-1.12123	-3.27736	-3.52856
H	-0.72296	-0.83724	-3.41555
N	0.36365	0.52198	-1.46601
H	1.30467	-3.56062	1.47199
H	0.79908	-5.95954	1.38990
H	-0.33889	-6.94721	-0.59464

H	-0.99596	-5.49424	-2.48803
S	1.30892	3.50375	-0.66228
O	1.22547	3.03204	-2.07076
O	1.11458	2.35574	0.30753
O	0.58374	4.72602	-0.31674
C	-5.41860	0.31486	0.24422
C	-5.61202	-0.42621	1.41584
C	-6.41481	0.07421	2.44011
C	-7.03200	1.31957	2.30241
C	-6.84451	2.05792	1.13370
C	-6.04142	1.55780	0.10751
C	-4.52636	-0.22223	-0.87882
H	-5.13064	-1.39369	1.52652
H	-6.56352	-0.51081	3.34326
H	-7.66003	1.70785	3.09890

Reference

Gaussian 09, Revision D.01,M. J. Frisch, G. W. Trucks, H. B. Schlegel, G. E. Scuseria, M. A. Robb, J. R. Cheeseman, G. Scalmani, V. Barone, B. Menucci,G. A. Petersson, H. Nakatsuji, M. Caricato, X. Li, H. P. Hratchian, A. F. Izmaylov, J. Bloino, G. Zheng, J. L. Sonnenberg, M. Hada, M. Ehara, K. Toyota, R. Fukuda, J. Hasegawa, M. Ishida, T. Nakajima, Y. Honda, O. Kitao, H.Nakai, T. Vreven, J. A. Montgomery, Jr., J. E. Peralta, F. Ogliaro, M. Bearpark, J. J. Heyd, E. Brothers, K. N. Kudin, V. N. Staroverov, T. Keith, R. Kobayashi, J. Normand, K. Raghavachari, A. Rendell, J. C. Burant, S. S. Iyengar, J. Tomasi, M. Cossi, N. Rega, J. M. Millam, M. Klene, J. E. Knox, J. B. Cross, V. Bakken, C. Adamo, J. Jaramillo, R. Gomperts, R. E. Stratmann, O. Yazyev, A. J. Austin, R. Cammi, C. Pomelli, J. W. Ochterski, R. L. Martin, K. Morokuma, V. G. Zakrzewski, G. A. Voth, P. Salvador, J. J. Dannenberg, S. Dapprich, A. D. Daniels, O. Farkas, J. B. Foresman, J. V. Ortiz, J. Cioslowski, and D. J. Fox, Gaussian, Inc., Wallingford CT, 2013.